Review Article

Ayushi Rastogi, Kanchan Yadav, Archana Mishra, Manu Smriti Singh, Shilpi Chaudhary, Rajiv Manohar, and Avanish Singh Parmar*

Early diagnosis of lung cancer using magnetic nanoparticles-integrated systems

https://doi.org/10.1515/ntrev-2022-0032
received October 18, 2021; accepted January 2, 2022

Abstract: Lung cancer (LC) has high morbidity and fatality rate that can be attributed to its poor diagnostic and monitoring facilities. Hence, there is a need to design advanced detection and monitoring systems to facilitate fast, efficient, and early diagnosis. The emerging research on novel nanotechnology-based strategies and conceptual models has made early-stage detection of LC possible by employing magnetic nanoparticles (MNPs) to surmount the barriers of slow diagnostic efficiency. Herein, the emphasis is on the recent advancement of MNP-based detection and monitoring systems for LC diagnosis, and future perspectives in the current scenario are discussed. The integration of MNP-based advanced diagnostic tools (microfluidic chips, artificial intelligence, biosensors, biomarkers detection, machine learning, nanotheranostics, deep learning, and internet of things platform) with conventional ones bronchoscopy, computed tomography scan, positron emission tomography, distant metastases, transthoracic biopsy, and magnetic resonance imaging might help to resolve current challenges related to early diagnosis of LC.

Keywords: magnetic nanoparticles, functionalization, lung cancer, detection and monitoring based systems

*** Corresponding author: Avanish Singh Parmar,** Department of Physics, Indian Institute of Technology (BHU), Varanasi, Uttar Pradesh, India; Center for Biomaterial and Tissue Engineering, Indian Institute of Technology (BHU), Varanasi, Uttar Pradesh, India, e-mail: asparmar.phy@itbhu.ac.in
Ayushi Rastogi, Rajiv Manohar: Department of Physics, University of Lucknow, Lucknow, Uttar Pradesh, India
Kanchan Yadav: Department of Physics, Indian Institute of Technology (BHU), Varanasi, Uttar Pradesh, India
Archana Mishra: Nuclear Agriculture and Biotechnology Division, Bhabha Atomic Research Centre, Trombay, Mumbai, India
Manu Smriti Singh: Department of Biotechnology, Center for Nanosensor and Nanomedicine, Bennett University, Greater Noida, Uttar Pradesh, India
Shilpi Chaudhary: Department of Applied Sciences, Punjab Engineering College (Deemed to be University), Chandigarh, India

1 Introduction

Cancer is the world's largest cause of death, with approximately 10 million fatalities in the year 2020 [1]. Among the various cancers known, the major contributors are lung cancer (LC) (1.80 million deaths); colon and rectum cancer (0.94 million deaths); liver cancer (0.83 million deaths); stomach cancer (0.77 million deaths); and breast cancer (0.68 million deaths) [1]. According to the World Health Organization (WHO) estimate, a global death rate of 29.5 million is expected by 2040 [1,2]. The foremost risk factors of LC include chewing, smoking, tobacco, exposure to radioactive elements (asbestos), and harmful radiations (radon gas). Of all reported LC cases, almost 80% were diagnosed among smokers, consequently marking it the principal cause of death. The past ten years have shown radical transformation in clinical settings with respect to early-stage detection and monitoring of LC garnering more interest in the field as highlighted in various research articles [1–4]. However, the dynamic tumor landscape makes specific and early-stage detection and monitoring of LC more complex. Thus, there is a requirement to develop nanoparticle-based detection systems because these materials have high penetration capability in tissues. Definitely, early-stage LC diagnostics will be a key player in cancer management [5]. MNPs, which are drug-loaded, magnetically controlled, and targeted to diseased tissues, are being studied as a prospective therapy [6]. The blood–brain barrier, on the other hand, makes it difficult for MNPs to permeate the central nervous system (CNS) and reach the diseased tissue. Using a simplified geometrical model, computational fluid dynamics, and the discrete element approach, the recent article by Gkountas *et al.* [7] explores numerically the transport of MNPs over the barrier driven by normal pressure drop and external gradient magnetic fields. The permeability of the brain barrier was examined in relation to the nanoparticle size, external magnetic field, and blood flow in the channel. The findings show that applying a magnetic field improves drug delivery to the CNS. The permeability of larger MNPs (~100 nm) can

be enhanced by up to 30% when subjected to an external magnetic field; however, smaller MNPs (~10 nm) cannot be driven by the applied magnetic field and the permeability remains unaltered. Finally, the increased blood flow results in a 15% increase in permeability. Hence, it was concluded that the geometric properties of the endothelial cells, the nanoparticles' size, and blood flow are not as important as the external magnetic force for drug transport into the CNS.

LC is mainly classified into three types: (1) non-small cell lung carcinoma (NSCLC), (2) lung carcinoid tumor (LCT), and (3) small cell lung carcinoma (SCLC) with NSCLC as the predominant type comprising 85% of cases and the remaining 15% of cases fall under SCLC and LCT. In comparison to SCLC, is simple to identify and characterize NSCLC. NSCLC represents the malignant form of tumor and frequently arises in the lung peripheral tissues. In the year 1943–1952, Denoix first proposed the LC staging as per the standard "Tumor-Node-Metastasis" classification. It differentiates the LC stages based on the tumor size as "TX," "T0–T4;" number of nodes "N0–N3;" and degree of metastases "M0, M1a, and M1b" [3]. On the other hand, SCLC is a considerably more severe kind of cancer of LC than NSCLC because the rate of proliferation of malignant cells into other body parts of SCLC patients is much higher than in patients diagnosed with NSCLC. The fundamental difference between SCLC and NSCLC is related to the malignant tumor size and the proliferation rate of these cells. Oncologists widely use this classification for diagnosing different stages of LC. According to the WHO study, there is no recognized histological grading system set up for early diagnosis and monitoring of LC; nevertheless, the grading system for neuroendocrine tumors categorizes them as low-grade tumors, intermediate-grade tumors, and high-grade tumors [3]. Most lepidic cancers are classified as low-grade tumors; however, large cell carcinoma is usually categorized under high-grade tumor type [4]. The majority of SCLC metastases occur in the main and secondary bronchi.

This review article highlights the use of magnetic nanoparticles (MNPs) as diagnostic and monitoring tools for early detection of LC and a concise view of the challenges involved in this field. There are considerable reviews of literature covering research on MNP-based cancer diagnosis [8–12]. However, this review presents a concise classification of different types of MNPs with their unique features and limitations as shown in Table S1 (provided in Supplementary). In short, it will be helpful for the readers to understand the use of advanced technologies such as artificial intelligence (AI), machine learning (ML), deep learning, internet of things (IoT), *etc.* [10,13–15] in solving the current challenges involved in the early diagnosis of LC. The preliminary section of this review highlights the role of MNPs and their importance in the biomedical field. The second section explains the classification of MNPs, their synthesis and functionalization methods, unique features and limitations [16–67]. In this section, the role of MNPs in biomedical and clinical diagnostic applications based on unique properties such as superparamagnetic, nontoxic, biocompatible, chemically inactive and environmentally friendly have been discussed. The ease of tunability and the customized surface of conjugated MNPs make them a suitable choice for synthesizing novel MNPs for diagnostic applications [10,11]. MNPs serve as an antimicrobial agents, anticancer agent and contrast agents in targeting, imaging, diagnosis, and hyperthermia [12]. Nonetheless, various parameters must be considered while evaluating the treatment, including temperature dependency over time, treatment period, tumor form, tissue damage, and nanoparticle dose. Polychronopoulos *et al.* [68] recently published a computer model aimed at determining such parameters, especially for ellipsoidal (prolate and oblate) tumors with a variety of aspect ratios. The model is simple to use and duplicate for a variety of treatment settings, and it might be valuable for future therapy planning. In Section 3, conventional diagnostic and monitoring systems based on MNPs have been elaborated, which encompasses bronchoscopy, computed tomography (CT), magnetic resonance imaging (MRI), distant metastases and transthoracic biopsy and positron emission tomography (PET) [12,16]. Although healthcare workers and professionals routinely perform the aforementioned means of diagnosis, however, conventional techniques are not up to the mark with respect to precision and sensitivity in tumor diagnosis. This leads to poor patient compliance and chances of false-positive results if the equipment is not properly cleaned and sterilized adequately between subsequent analysis [10]. Hence, there is an urgent need to integrate these conventional diagnostic tools with advanced diagnostic and monitoring systems such as biomarkers detection, microfluidic chips, biosensors, nanotheranostics, AI, and wearable devices that form part of Section 4 [9,13–15,69–71]. The limitations of each one of these systems have been discussed. The concluding section of this review recapitulates the future challenges and refinements required in MNP-based diagnostic and monitoring systems for the early diagnosis of LC. Although the combination of conventional and advanced diagnostic methods helps in resolving various diagnostic issues, there are still numerous proposed challenges that are yet to be resolved in future.

2 MNPs

The emergence of MNPs in diagnostics and monitoring systems has gained a lot of interest globally [8]. The unique features and high penetration capability of MNPs offer a significant advantage in tumor targeting and imaging [12,16]. Moreover, MNPs can function as direct diagnostic agents due to their inherent superparamagnetic properties [22]. Among all nanoparticles known so far, MNPs have gained immense attention in oncology because of their unique pharmacokinetic properties, MRI contrast, simple and scalable synthesis, easy surface modifications, low toxicity, and biocompatibility that assist them to serve as outstanding material for LC diagnosis [16–67]. The magnetic characteristics of MNPs are determined by the core area in such a way that the superparamagnetic nature is shown by particle sizes up to 100 nm, making it dimension dependent. MNPs are typically smaller or comparable in length to organic units, ranging from a few nanometers for proteins and genes to nanometer loads for viruses and up to 100 nm for cells [41]. MNPs are beneficial because of their small size, which allows greater circulation and precise distribution within the network or near the targeted site. Table S1, provided in the Supplementary information, lists the classification of different types of MNPs with their synthesis methods (details of each method can be found in Table S2 provided in the SupplementaryInformation), structural characterization, unique features, and limitations. However, because the internal structure/cores of MNPs are generally composed of iron (Fe), cobalt (Co), and nickel (Ni), which are noxious to cells and therefore are safer core materials (magnetite [Fe_3O_4] or maghemite [$-Fe_2O_3$]), as well as a variety of biocompatible shells to cover the noxious cores are put into use (Table S3 provided in Supplementary information and Table 1). Other fluorescent markers, such as fluorescent protein molecules, luciferase, and fluorescent dyes tagged on the surface of MNPs, can also be used as contrast agents in addition to magnetic cores. As a result, optical imaging techniques can employ these fluorescent markers. The benefits and drawbacks of various imaging techniques are summarized in Table 2 as explained by Cores *et al.* [41].

MNPs as drug delivery vehicles were initially proposed in the 1970s [72]. The magnetic drug targeting (MDT) approach is a useful method for directing cells or cell components to their intended sites. To accomplish this, MNPs are frequently employed to label cells *via* co-incubation. MNPs can pass through the cell membrane in three ways: external binding (antibody-mediated), endocytosis, and passive diffusion [41]. Magnetized cells would be specifically directed to injured sites using magnetic

Table 1: Clinically recognized IONP-conjugated pharmaceuticals with biomedical platform applications [12]

Serial No.	Chemical compound name	Coating	Application	Clinically recognized	Ref.
1.	Ferumoxtran (Combidex®)	Dextran	Macrophage imaging, Lymph node imaging, cell labeling, CNS imaging, blood pool agent, MRI	For trials in the clinic	[57,58]
2.	Ferucarbotran (Resovist®)	Carboxydextran	Cell labeling, MRI, liver imaging, CNS imaging	Accepted	[59–61]
3.	Ferumoxide (Feridex)	Dextran	Cell labeling, liver imaging, MRI, CNS imaging	Market access revoked	[62–64]
4.	Feruoxytol (Feraheme®)	Carboxymethyl-dextran	In patients with severe renal disease, iron replacement treatment is used	Accepted	[65]
5.	Ferglose (Clariscan™)	PEGylated starch	MRI, Blood pool agent	For trials in the clinic	[66]
6.	Feruoxsil (Gastromark®)	Siloxane	Oral GI imaging	Accepted	[67]

Table 2: Pros and cons of various imaging methods and contrast agents applied for *in vivo* cellular imaging and tracking. Reprinted with permission from ref. [16]

Imaging techniques	Contrast agents	Advantages	Disadvantages
MRI	SPIONs	3D scanning of the whole body, painless, without the implication of ionizing radiation, cell quantification is challenging but feasible, external magnetic field used to modify cells	Patients with implants are not suitable for this treatment, cell division results in tracer dilution, potential agent transfer to other cells, it is possible that the imaging procedure will make the person feel claustrophobic
MRI	Fluorescent agents, perfluorocarbon, and gadolinium	3D scanning of the whole body, without the implication of ionizing radiation, individual cell detection is achievable	Patients with implants are not suitable for this treatment, cell division results in tracer dilution, potential agent transfer to other cells, it is possible that the imaging procedure will make the person feel claustrophobic
Optical	Luciferase substrates, protein fluorescent markers, near-infrared fluorophores, and fluorescent dyes	The use of a huge proportion of fluorophores allows for simultaneous examination of several cell types and lineages, and it may be coupled with other imaging modalities. It also avoids the use of ionizing radiation	Cell division results in tracer dilution, dye cytotoxicity, limited tissue penetration depth
PET and spectroscopy (SPECT)	PET: high-energy positron emitters; SPECT: high-energy gamma emitters	Highly elaborative, 3D scanning of the whole body, no tracer signal dilutions with transgenic methods because there are no cell division dilutions, quantification feasibility with SPECT	Quantification can be challenging in PET, ionizing radiation, intravenous injection of contrast agent, stem cells are genetically modified, an allergic response to radioactive tracer might be possible
Ultrasound	Microbubbles	Detection of single cells without the use of ionizing radiation, imaging of soft tissues, relatively inexpensive, fast	Limited to specific body parts, low resolution, challenging quantification, cell division results in dilution of contrast agent and can transfer to other cells
X-ray and CT	High-density gadolinium or iodine	CT allows whole-body scan, 3D imaging, relatively inexpensive, and fast	Too high concentrations of contrast agent can be noxious, it is difficult to quantify X-ray data, increased risk of developing cancer at a later stage, ionizing radiation in dyes

force if an external static magnetic field is applied. As shown in Figure 1(a), an electromagnet and a high magnetic flux density were used to create a strong magnetic field with a gradient of up to 72 T/m at the pole tip [6]. Chemotherapeutic or anticancer drugs were attached to MNPs, and the resulting ferrofluid solution was injected into an artery and delivered directly to the tumor location. An external magnetic field concentrates the particles and medications connected to them at the specific tumor site (Figure 1(a)) [6]. According to Dames *et al.* [73], aerosol droplets containing MNPs (Figure 1(b)) might be utilized to route medications to specific parts of the lungs, similar to "traditional" MDT (Figure 1(a)) [74]. The aerosol droplet is the real medication carrier. As a result, unlike "traditional" MDT, the medication does not need to be attached directly to the MNPs, removing the risk of drug desorption from the particle during delivery or in the target tissue. In this instance, the MNPs need not be customized for each medicine under consideration [74]. Because MNPs are known to be effective MRI contrast agents, MRI can detect the migration of magnetically targeted cells. Abdeen and Praseetha [75] found that in the presence of a magnetic field heat was generated due to the oscillating effect of MNPs and the generated heat reduced the growth of the tumor. This observation shows that future studies will focus on the MNP pharmacokinetics to ensure enhanced permeability and retention effect (EPR). Fallahzadeh *et al.* [76], proposed that future research will focus on the favorable response of the patient's body to MNPs. Improving early cancer detection methods and anticancer medication

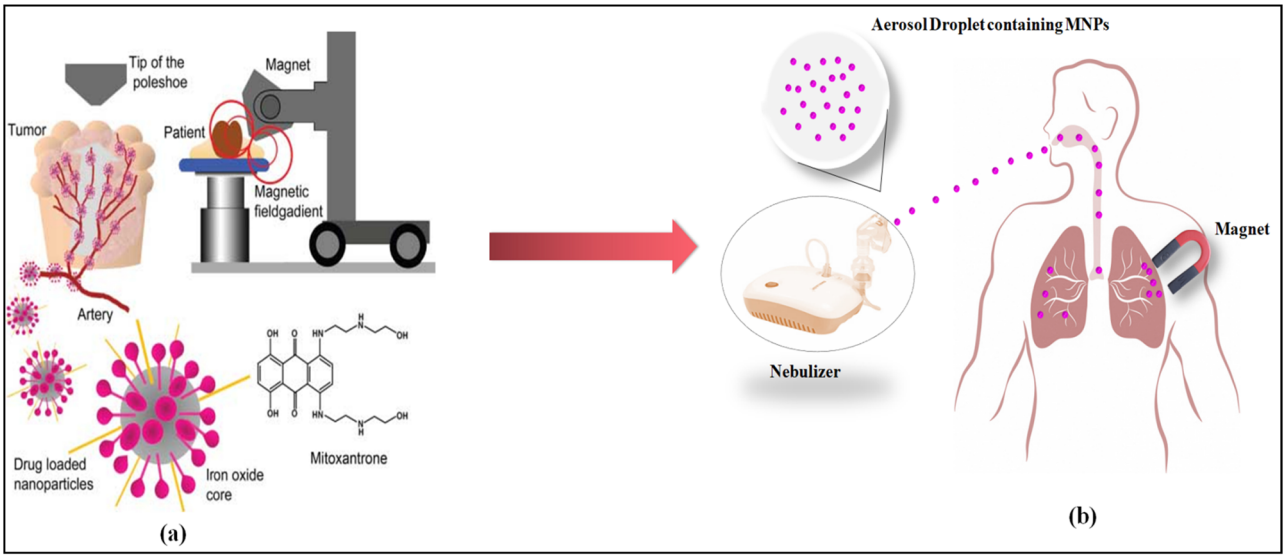

Figure 1: (a) MDT with intravascular administration. MNPs bind effectively to an anticancer drug that is directly injected into the tumor-feeding blood vessel of the patient. It is then concentrated in the target tumor site by an external magnetic field. Reprinted from ref. [6] by Creative Commons License. (b) Targeted delivery of magnetic aerosol droplets. Reprinted from ref. [74] by Creative Commons License.

administration by blending functionalized superparamagnetic MNPs to the tumor site is one of the most widely pursued areas of research. Superparamagnetic iron oxide nanoparticles (SPIONs) induced hyperthermia treatment can destroy malignant tissues all over the body [77–79].

2.1 Classification, synthesis, and functionalization of MNPs

MNPs are categorized into the following types:

(1) Metals and their oxides (Fe, Co, Ni; Fe_3O_4, Fe_2O_3, NiO).
(2) Alloys (FePt, FePd).
(3) Ferrites ($CoFe_2O_4$, $MgFe_2O_4$, $MnFe_2O_4$, $ZnFe_2O_4$, $NiFe_2O_4$, $CuFe_2O_4$).

SPIONs belong to a ferrimagnetic group of MNPs with broad significance in the areas of biomedicine and bioengineering. While several SPION-based diagnostic methods are under clinical and preclinical investigation, others have been already commercialized for diagnostic purposes (Table 1). Fe_3O_4, γ-Fe_2O_3, and α-Fe_2O_3 are a few examples of SPIONs [20]. The presence of ferric ions (Fe^{2+} and Fe^{3+}) has resulted in the dominance of SPIONs for utilization in biomedical applications. Different types of MNPs with their synthesis methods and unique features are elaborated, as shown in Table S1. The synthesis of MNPs has been achieved by diverse processes as listed in Tabe S2. A number of these processes have led to extraordinary properties like monodispersity, shape control, and stabilization. Co-precipitation or hydrothermal synthesis, as well as the sol-gel technique, are the most widely employed methods. Thermal breakdown, microemulsion, sonolysis, and biosynthesis are examples of some novel and modern techniques. The type of MNPs has a greater influence on the optimal synthesis pathway. The most used MNPs for diagnostic purposes are often spherical in shape. However, researchers have investigated different morphologies that imparted additional features to the nanoparticles such as hollow rod shape for drug delivery [80] and nanocubes for guided chemotherapy and photothermal therapy (PTT) [81].

2.2 Functionalization of MNPs

Functionalization of MNPs is required to improve their applicability for further applications. Functionalization is the process that involves the addition of new features, properties, and functions to a material by changing its surface chemistry [8,82–85]. This is a fundamental method used throughout materials science, chemistry, pharmacy, textile industry, bioengineering, nanotechnology, and biomedicine. Since the cores of MNPs are made up of toxic materials, hence it is required to reduce their toxicity for targeting and imaging purposes. To achieve this, the bare cores of MNPs are covered with biocompatible capping agents that act as shields/shells to lower their toxicity. For example, nanoshells that have been used as dielectric cores usually made up of silicon (Si), are coated with a thin

layer of the shell (gold or Au) surrounding them. It has a size range between 10 and 300 nm [86]. The working principle of these nanoshells involves the conversion of electrical energy mediated by plasma into photon energy that can be optically tuned through UV-IR emission/absorption arrays. Although the large-size nanoshells have limited usage, they are desirable because of their imaging process and are being devoid of heavy metal toxicity [87]. Both active and passive ways of targeting cells by Au nanoparticles were demonstrated in the research conducted by Nunes *et al.* [87,88]. The working principle of passive targeting has been mediated by the assembly of Au nanoparticles to enhance imaging by permeability and retention effect (EPR) in tumors [88]. On the other hand, for active targeting, Au nanoparticles get coupled with tumor-targeted specific drugs. Earlier findings have significantly influenced the early diagnosis of cancer because these allow the detection of small tumors of millimeters (mm) size in the patient's body [87]. By using a one-step solvothermal method, Qian *et al.* [89] synthesized Fe_3O_4 nanospheres/reduced graphene oxide (rGO) nanocomposites. In contrast to Fe_3O_4 microspheres/rGO and Fe_3O_4 nanopolyhedrons/rGO, the resultant nanocomposites had the most peroxidase-like activity toward the usual peroxidase substrate (3,3′,5,5′-tetramethylbenzidine) oxidation. This suggests that using their peroxidase-like catalytic activity, selective synthesis of Fe_3O_4/graphene composites with desirable properties is crucial. Based on their high activity, the Fe_3O_4 nanospheres/rGO nanocomposites were used to construct an economical colorimetric platform for the sensitive and selective detection of acetylcholine. Gao *et al.* [90] described the synthesis of MNPs coated with chitosan (CSMNPs) for use in a capture detection immunosorbent assay in which antigen may be collected, sorted, and enriched prior to the assay method. The carcinoembryonic antigen (CEA) was identified by CSMNPs with a LOD of up to 1 ng/mL. Chitosan was employed as both a ligand and a surface-modifying agent in a one-step solvothermal method to make CSMNPs. The presence of surface amine groups in CSMNPs provided high dispersibility in aqueous solution as well as suitable locations for covalently attaching antibodies to the MNPs. They also have catalytic characteristics for catalyzing color reactions in immunoassays, as well as magnetic properties for capturing, separating, and enriching antigens prior to the assay procedure. Table S3 in Supplementary shows different types of capping agents that serve as shell material to coat MNPs. The motif of coating MNPs with capping agents is to improve its applicability by preventing aggregation of MNPs and to provide protection to cells from toxic cores. This can be attained by the proper choice of shell materials that are hydrophilic in nature (e.g., silica) and allows diffusion of MNPs in a liquid environment. The three most important methods of functionalization include [8,82–85] the following:

(1) Ligand addition and functionalization *via* bioconjugation.
(2) Ligand-exchange strategy to MNPs.
(3) Coating of hydrophilic materials like silica.

2.2.1 Ligand addition and functionalization *via* bioconjugation

The stabilization of MNPs can further be increased by coating organic and inorganic materials. The presence of hydroxyl groups (–OH) of nanoparticles produced by coprecipitation or other synthetic techniques might readily explain functionalization *via* bioconjugation at the MNP surface. Depending on the pH of the medium, it can be positively or negatively charged. If the –OH ligands are free, nonpeptizable particles will be produced at pH 7.5; however, ligands stay linked to MNPs in the pH range of 6–10. As a result, the free hydroxyl groups on the surface of MNPs help in the binding with biomolecules. Some of the clinically approved iron oxide MNP (IONP)-conjugated compounds with their applications are listed in Table 1, and the summarized form of MNPs as nanocarriers for cancer diagnosis is shown in Figure 2.

IONPs/SPIONs are usually stabilized by the addition of stabilizers or surfactants like oleylamine and/or oleic acid that are generally hydrophobic. Now, these nanoparticles are often made hydrophilic for biomedical applications by functionalizing their surface *via* surfactant/ligand exchange or stabilizers [8,82–85]. The addition of surfactant is achieved through the adsorption of the amphiphilic molecules on the nanoparticle surface that contains both hydrophobic and hydrophilic segments [82]. A double-layer structural arrangement is formed by the hydrophobic component with the initial hydrocarbon chain, while there is an exposure of hydrophilic groups outside of the nanoparticles that render them to be dispersed in water easily.

2.2.2 Ligand-exchange strategy

Ligand-exchange strategy is achieved through the presence of a new bifunctional surfactant or ligand in place of the original surfactant by direct replacement process [85]. This bifunctional surfactant/ligand has at least two functional groups attached to it such that one of them is capable of tightly binding to the nanoparticles' surface *via* a strong chemical bond and the other functional

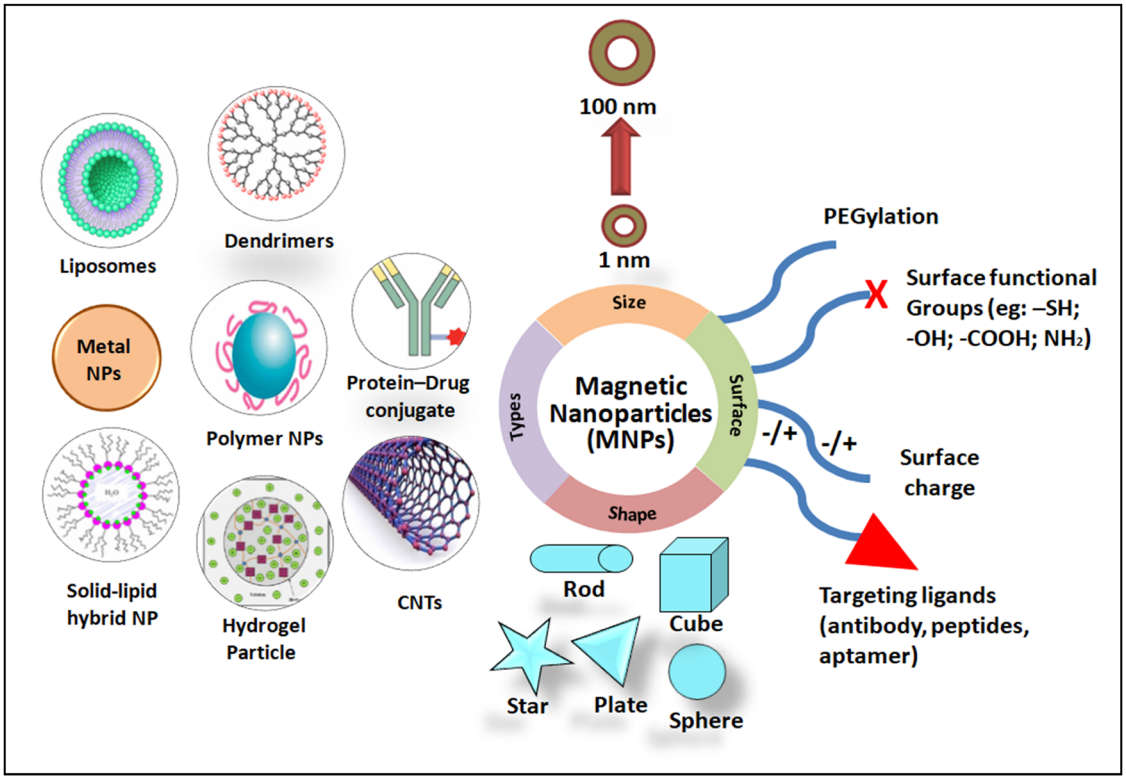

Figure 2: Classification of MNPs employed as carriers for drug delivery in cancer therapy [8].

group present at the opposite end is polar in nature and makes the nanoparticles disperse in water easily or be further functionalized in a physiological environment. The strong interaction between the bidentate/multidentate functional groups and the MNP surface can be achieved through the bifunctional ligand-exchange strategy that provides better colloidal stability under physiological conditions as compared to the amphiphilic micelle coating method. The development of the bifunctional ligand-exchange strategy [85] was made for the replacement of hydrophobic ligands present on MNPs with organosilanes that possess different functional groups [82]. These organosilanes feature alkoxyl moieties that establish a covalent connection with surface hydroxyl groups (–OH) *via* esterification or dehydration to link with the metal oxide. Amino ($-NH_2$)-, carboxylic acid (–COOH)-, and polyethylene glycol ($C_{2n}H_{4n+2}O_{n+1}$)-terminated silanes have been discovered to render MNPs extremely water-soluble and stable.

Different types of functionalizations of MNPs are shown in Table S3, which include

(1) Core/shell MNPs [8]
(2) Polymeric MNPs [8]
(3) MNPs entrapped in polymeric films [8]
(4) Magnetic heterodimers functionalized with two different functional units or biological species [40]
(5) MNPs modified with lipid mono- and bilayers [40].

Heterodimers are created when two distinct nanoparticles (for example, magnetic and metal or semiconductor) are combined in a single nanoassembly where the particles are bonded to each other, resulting in a unique multifunctional species [40]. The two nanoparticles in this species are made up of two separate materials with distinct characteristics, like “Siamese twins” (dumbbell-like bifunctional particles). Controlled development of a second particle close to the original particle is used to link two nanoparticles in a single composite assembly. MNPs, Fe_3O_4 or FePt (8 nm), with a stabilizing organic shell composed of a surfactant, were distributed in an organic solvent (dichlorobenzene) and added to an aqueous solution of Ag^{2+} salt, as explained by Katz [40]. Micelles containing self-assembled MNPs (on the liquid/liquid interface) were obtained by ultrasonication of this bi-phase organic solution. The Ag^+ ion is next penetrated through defects in the surfactant shell, where it is catalytically reduced by Fe^{2+} sites to generate Ag nanoparticle seeding. Further reduction of Ag^+ ions on the Ag seed caused seed development and the production of Ag nanoparticles on one side of MNPs, resulting in twin particles. In a similar manner, another Ag nanoparticle was created on the FePt

MNP side. Using the difference in surface characteristics of the two portions of the produced heterodimeric nanoparticles, the two components of the dimer may be easily changed using various chemicals.

3 Conventional diagnostic methods for LC detection

3.1 Bronchoscopy

Bronchoscopy is an invasive technique that involves introducing a camera-connected illuminated tube (Bronchoscope) into the patient's lungs through the nose or mouth [71]. As the bronchoscope exposes the interior tissues, bronchi, and bronchioles, it is possible to identify many abnormalities in the lungs, such as tumors, signs of infection, and excess mucus, using bronchoscopy. Rigid and flexible are the two different forms of bronchoscopy [71]. Rigid bronchoscopy uses a bigger, more rigid piece of equipment to access the proximal airways. It is usually done to remove foreign objects and airway stents in order to manage severe hemoptysis. Also, it has application in tumor debulking and airway dilatation [91]. Flexible bronchoscopy, on the other hand, accesses the lower airways using a smaller, more flexible piece of equipment. Bronchoscopy is commonly suggested for the early detection of LC because it provides a thorough review of distinct characteristics of the lungs from the inside [92]. Fiber-optic bronchoscopy is extensively utilized in practice because it is safe (0.12% complication rate) and simple to conduct [93].

3.1.1 Autofluorescence bronchoscopy (AFB)

AFB is a form of flexible bronchoscopy based on the finding that when dysplastic or carcinomatous lesions occur, the emission spectrum of the bronchial mucosa alters under blue light [69]. Normal bronchial mucosa appears green after image processing, whereas dysplastic/carcinomatous tumors appear reddish brown. The fundamental rationale for utilizing blue light is to distinguish between normal and cancerous tissue based on color alone, without the addition of any fluorescence-enhancing drugs. The white field is more specific, while AFB is more sensitive, with bronchitis being the most common confounder for AFB [94]. AFB is most suited for in situ application in squamous cell carcinoma, which is an uncommon occurrence, restricting its use. It has, however, been included as part of the work to be done in the LungSEARCH research [94], a multicenter clinical trial for the early identification of LC. The combination of AFB with other current techniques, such as white light bronchoscopy or CT scans (Section 3.5), can considerably enhance the early diagnosis of LC.

3.2 Endobronchial ultrasound (EBUS)

EBUS is a minimally invasive technique that is used to identify a variety of lung diseases [71]. The interior tissues and the airwall of the lungs are seen using EBUS in conjunction with routine bronchoscopy [95]. EBUS is widely applied in normal practice for early identification because of its low risk and high diagnostic value. Linear EBUS and radial EBUS are the two EBUS systems available [93]. The ultrasonic transducer is utilized in the distal end of linear EBUS to visualize the curvilinear pattern of the airways using a fixed array. A mechanical radial microprobe is utilized in radial EBUS to visualize the characteristics of the lungs' periphery. EBUS, in combination with frequent bronchoscopy, has been shown to be a highly successful technique for detecting the degree and depth of invasion in the LC.

3.3 Confocal endoscopy

Confocal endoscopy, also known as confocal laser endoscopy (CLE), is a cutting-edge imaging method that allows for real-time imaging of cellular and subcellular features in the mucosa and live cells in the lung tissue [71]. CLE might be used to investigate the architecture of alveolar elastic fibers, microvessels in lung tissues, and bronchus mucous membranes. For the reliable diagnosis of LC, Comino *et al.* [96] investigated probe-based CLE (pCLE) combined with computer-aided diagnostics techniques. The obtained data were used to study the deep-learning feature spaces to provide improved CLE pictures (83.4% accuracy) of lung tissue neoplastic cells.

3.4 Biopsy

Lung biopsy is a procedure that involves removing a sample of tissue from the lungs for evaluation. A specific biopsy needle or surgery is used to remove a tiny portion of the lung. A tissue biopsy is a sort of biopsy that is

utilized to detect several lung diseases, including LC [71]. To identify lung disorders, many types of biopsies are available [71]. A needle biopsy, for example, involves inserting a needle into the lung and extracting a sample. A bronchoscope (a long, thin tube with a small camera) is used to perform a transbronchial biopsy. The thoracoscope, which transmits the chest picture to the computer monitor, is used in video-assisted thoracoscopic surgery. The thoracoscope is inserted into the chest cavity through a tiny incision in this minimally invasive procedure. Open biopsy, on the other hand, necessitates a bigger incision in the patient's skin in order to access and remove a tiny section of the lung for further investigation. For years, tissue samples have been used to detect/diagnose LC; however, their invasive nature restricts its utility.

3.5 CT

In radiology, CT is used to obtain detailed pictures of the body in a noninvasive manner [12]. CT scan uses a spinning X-ray tube and detectors to measure the X-ray attenuations of various tissues inside the body. X-ray readings are often obtained many times from various angles and then processed on a computer to reconstruct the algorithms for creating tomographic pictures of the body. Contrast agents (iodine- and gadolinium-based contrast agents are the most common ones) for CT are administered intravenously. On the other hand, patients with renal impairment have been documented to be extremely susceptible to widely used contrast agents because they cause toxicity in cells and tissues. As a result, MNPs were considered as a possible replacement for iodine-based contrast agents [97,98].

In CT imaging, gold-coated iron oxide glycol nanoparticles can be employed as a contrast agent [12]. It was discovered that nanoscale MNPs are extremely biocompatible, biodegradable, and have X-ray attenuation properties, as well as pose a minimal toxicity risk when exposed to low levels over time. They are a good candidate for CT and MRI imaging because of these features [99,100]. Naha *et al.* [99] synthesized a nanocomposite of bismuth-IONPs with a dextran covering and tested the nanoconjugate's cytotoxicity, accumulation, and half-life. HepG2 (human liver cancer cell line) showed less cytotoxicity, and CT imaging was used to examine the contrast in blood arteries and the heart following overnight incubation with nanoparticles. The nanoconjugate was discovered to have high X-ray attenuation, a long circulation half-life in the body, and biocompatibility, which makes it a promising candidate for use as a CT and MRI contrast agent.

Reguera *et al.* [101] synthesized Janus MNPs that were employed as a contrast agent in a range of techniques including CT, MRI, TEM, PAI (photo acoustic imaging), surface-enhanced Raman spectroscopy (SERS), and optical imaging. The results showed that these can collect the most cellular information, which make them an excellent imaging tool in the biomedical platform [101]. On the other hand, the negative consequences of ionizing radiation might occasionally limit their usage in patients.

3.6 PET

PET is an imaging technique wherein radioactive materials known as radiotracers are employed to envision and determine the changes in metabolic reactions [70]. Radioisotopes used in PET imaging possess a short half-life with ^{11}C of 20 min, ^{13}N of 10 min, and ^{15}O of 2 min. ^{64}Cu was widely studied due to its half-life up to 12.7 h. Researchers found that cross-linked dextran nanoparticles had a noteworthy affinity to tumor-associated macrophages [102,103]. ^{64}Cu-labeled dextran nanoparticles by macrocyclic chelators can be applied in PET imaging for clinical oncologic diagnosis. However, the poor stability of radiometal chelator complexes *in vivo* [104] greatly influenced the physicochemical properties of nanoparticles in PET imaging. Hence, the chelator-free ^{64}Cu nanoclusters were developed through a simple one-pot chemical reduction method by employing bovine serum albumin as a framework for PET LC detection to improve the stability and accumulation [105]. Although Cu-based radionuclide has been studied extensively and made some progress, the blemishes of its instability and higher accumulation in the liver are still the focus of lung diagnosis studies.

3.7 MRI

In vivo imaging of the cells is required to track and monitor disease treatment, immune cell distribution into the body, diffusion time, proliferation, and migration rate. PET, CT, and MRI are some of the imaging methods utilized for this purpose [12,70]. MRI, in particular, has been demonstrated to have a high spatial resolution [106], making it an excellent imaging method for *in vivo* imaging studies. It is a high-resolution imaging method that uses a strong magnetic field and radio waves to create pictures of numerous

organs in human and animal bodies. In experimental contexts, it has been frequently utilized in clinical radiology with nonionizing radiation. In addition, the modality is tomographic, allowing for high-resolution soft tissue penetration. The magnetic field, radio waves, or electric fields are used in MRI to show the body's precise interior structure. T1 and T2 contrast agents are the two types of MRI contrast agents [12]. T1 agents affect water protons' longitudinal relaxation time, whereas T2 agents affect their transverse relaxation time. It shortens the T1 and has a mild influence on T2, resulting in a brighter picture when positive T1-weighted. Negative T2/T2*-weighted contrast, on the other hand, reduces T2 relaxation time and results in dark pictures [107]. Because of their superparamagnetic characteristics, MNPs lower the relaxation period of surrounding protons, making them good candidates for MRI contrast agents.

MRI cannot yet be directly applied in LC detection due to the motion artifacts, numerous susceptibility gradients, and low proton density [108]. By combining with the optimized proton MRI sequences based on ultrashort echo time (UTE), ultrashort echo-time magnetic resonance imaging (UTE-MRI) can be applied in lung tissue imaging [109]. Gadolinium is clinically used as the MRI contrast material, showing the noninvasive detection of NSCLC by UTE-MRI that can be achieved *via* the orotracheal administration of nebulized gadolinium nanoparticles with the enhanced signal. Moreover, gadolinium can be selectively deposited in tumor tissues while removed by healthy tissues [110]. Accurate and detailed detection information can be obtained through the simultaneous usage of two MRI contrast agents [70]. Longitudinal relaxation contrast medium (T1 contrast medium), such as Gd-DTPA and Mn-DPDP, and transverse relaxation contrast medium (T2 contrast medium), such as superparamagnetic iron oxide, among which T1 contrast medium can effectively decrease the T1 relaxation time by interactions with the neighboring T2 contrast medium [70]. The strong magnetic coupling between the T1 and T2 contrast medium could disturb the relaxation effect of the paramagnetic T1 contrast medium, leading to an undesirable weakening and quenching of the magnetic resonance signal. According to this, a smart MRI contrast agent with Fe_3O_4 nanoparticles in core (T2 contrast medium) and the silica shell containing water-soluble Mn-porphyrin (T1 contrast medium) and anticancer drug doxorubicin in the shell was constructed (Figure 3(a)) [111]. After the mod-

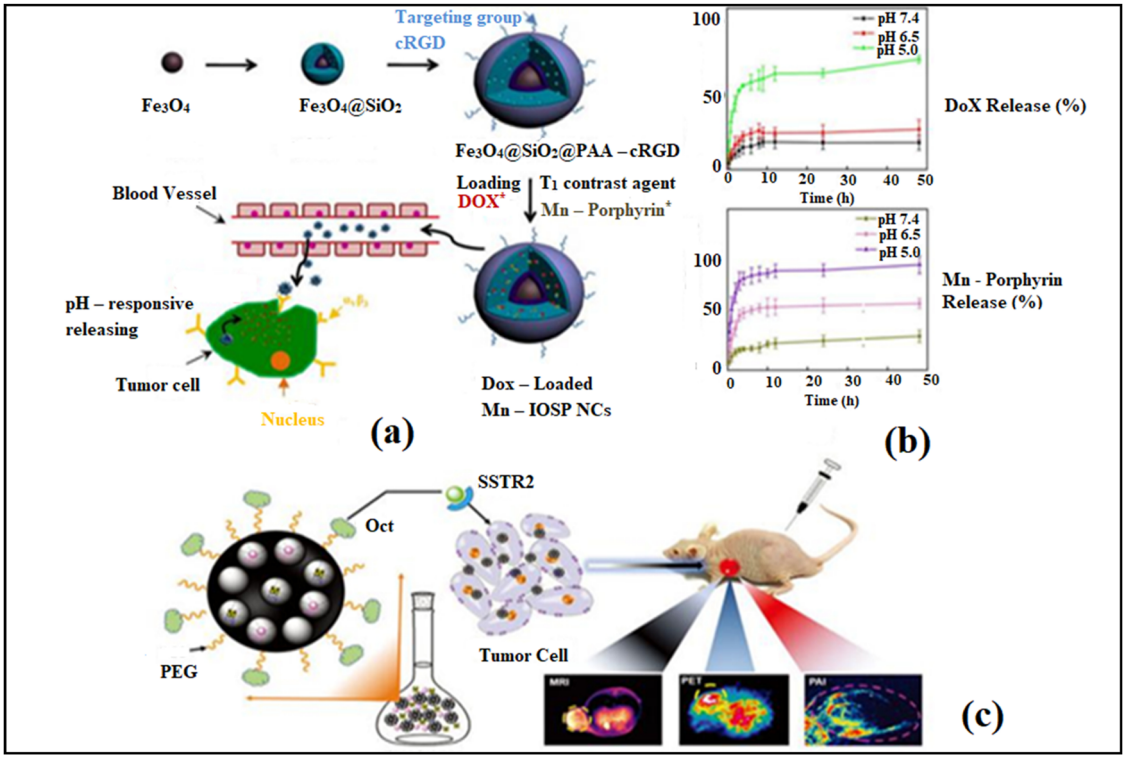

Figure 3: (a) Schematic presentation of synthesis, release, and imaging process of Fe_3O_4@SiO_2@PAA-cRGD. Reprinted from ref. [111] by Creative Commons License. (b) Drug release study using UV-Vis spectra. Reprinted from ref. [112] by Creative Commons License. (c) Schematic presentation of the synthesis of contrast agent and imaging mode (MRI/PET/PAI). Reprint from ref. [70] by Creative Commons License.

ification by poly(acrylic) acid (PAA) and c(RGDyK) peptides (cRGD), the dual-mode MRI contrast medium was equipped with functions of tumor-specific target and pH response (Figure 3(b)) [112]. When the contrast medium was internalized by cancer cells, the tumor acidic microenvironment facilitated the release of porphyrin and recovered the quenched signal caused by the combination of Fe_3O_4 and Mn-porphyrin (Figure 3(a)) [111]. Compared to single-contrast medium imaging, multimodal imaging with several contrast mediums can provide complementary imaging information for cancer diagnosis. Co-delivery of various contrast mediums without imaging signal interference is a great challenge. USRPs-Cy5.5 was constructed by covalently conjugating cyanine 5.5 on nebulized gadolinium nanoparticles for fluorescence tomography and UTE-MRI to detect LC noninvasively. Melanin nanoparticles in photoacoustic imaging (PAI) can be used as nanocarriers to codeliver ^{124}I (PET contrast agent) and Mn^{2+} (MRI contrast agent) by an electrophilic substitution reaction and a chelation reaction, respectively, which is an ideal vector for tri-mode imaging (Figure 3(c)) to improve the efficiency of LC diagnosis at an early-stage effectively.

3.8 Magnetic particle imaging (MPI)

MPI is a noninvasive tomographic method for detecting tracer particles with superparamagnetic characteristics. Diagnostics, imaging, and material characteristics are all areas where MPI might be useful. MPI may be used to create a signal by using nonionizing radiation to find and quantify the number of nanoparticles at any depth within the body. When superparamagnetic nanoparticles are magnetized, MPI signals are created, which are 107 times more sensitive than MRI signals. When SPIONs were used for lactoferrin conjugation, the magnetic particle spectrometer (MPS) provides the potential for 3D *in vivo* imaging with excellent spatial resolution [113]. A custom-built MPS was used to record the MPS signal [113,114]. Overexpressed cancer cells release particular proteases like trypsin and matrix metalloprotease-2 that can be identified by MPS. SPIONs were aggregated in the presence of biotin-labeled peptides, which were then preferentially recognized and broken by particular proteases contained in the peptides, causing the SPIONs to disperse. MPS signals detected the aggregation or dispersion state of SPIONs based on magnetic relaxation properties. As a result, MPS may be utilized in biomedical applications including fast detection of proteases in biological materials like tissue extracts, urine, blood, and cell culture medium for LC diagnosis [115].

4 Advanced diagnostic MNP-based systems for early detection of LC

The *in vivo* methods mainly include ultrasound-guided needle aspiration, transthoracic and distant metastases biopsy, AFB, EBUS, CT, PET, MRI, and other invasive biopsies, which can reflect the disease information by the visual image [69–71]. The anatomical structure and boundary range of the tumor can be seen clearly due to the ultrahigh resolution of MRI, but it was limited by a longer imaging time and the lack of molecular imaging information. Although PET imaging showed high sensitivity and provided systemic lesions information, it is still limited by insufficient spatial resolution and possible false-positive results caused by unsatisfactory specificity [12]. Low dose CT scans provide information to indicate the size, shape, and position of cancer cells in lymph nodes, but it has the disadvantages of low sensitivity and low specificity due to severe artifacts in pictures caused by internal organ motion and tattoos. Table 2 elaborates the pros and cons of different conventional diagnostic systems for early detection of LC.

To overcome the problems related to conventional diagnostics, the application of different kinds of functionalized organic and inorganic MNPs is considered in combating LC. The advanced technologies and machinery requirements could offer an effective route for the early diagnosis of cancer and cancer-related diseases. Advanced diagnostic tools for LC detection through MNPs include biomarkers [69], microfluidic chips [9], biosensors and aptasensors [10], nanotheranostics [10], AI, and wearable devices [13–15] as shown in Figure 4.

4.1 Biomarkers detection

In the area of LC detection based on MNPs, one vital step is biomarkers recognition. Cancer biomarkers are the molecular structures (aptamers, peptides, DNAs, proteins) responsible for disease development and its evolution. Therefore, the selection of these molecules is of crucial importance. Autoantibodies (AAbs), nasal signature, circulating tumor DNA (ctDNA), microRNA (miRNA), proteins, methylated DNA, and complement fragments are among the most common biomarkers [69,71]. There are several specific biomarkers depending on the type of LC, with the main biomarkers being CEA related cell adhesion molecule-1 (CEACAM), cytokeratin 19 fragment antigen 21-1 (CYFRA21-1), human epidermal growth receptor-2 (HER2), vasculo-endothelial growth factor receptors (VEGFR), epidermal growth factor

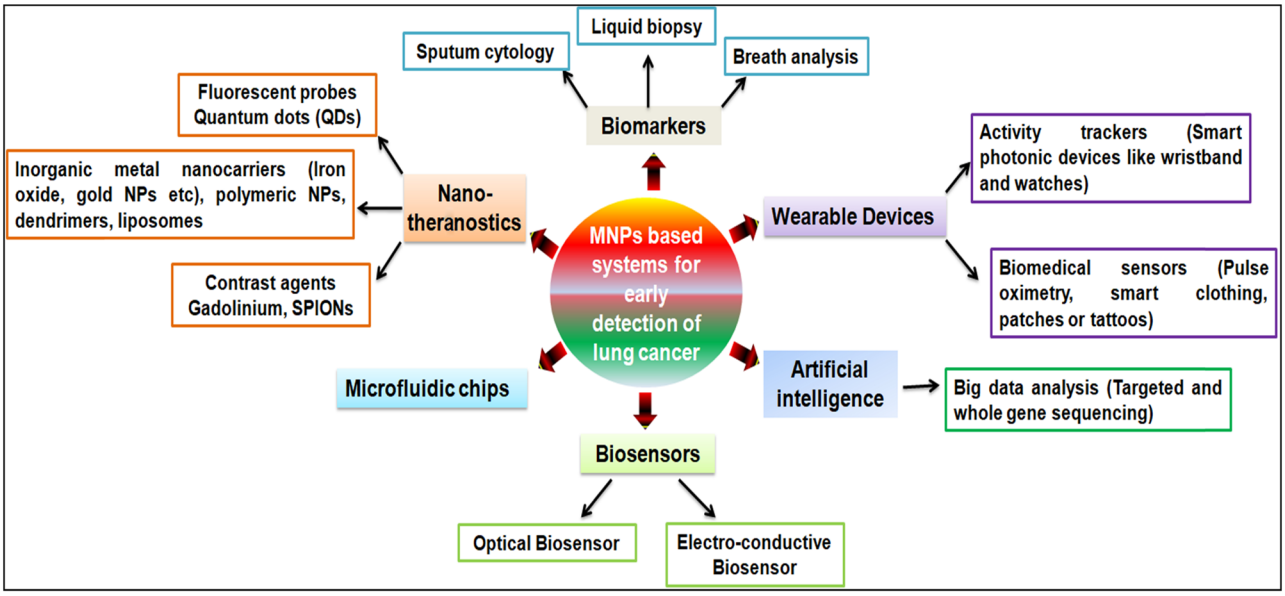

Figure 4: Advanced diagnostic tools for early detection of LC.

receptor (EGFR), class 1 phosphoinositide 3-kinase (PI3K), neuron-specific enolase (NSE), and V-raf murine sarcoma viral oncogene homolog B (BRAF) [10]. Protein and peptide-based biomarkers identified in blood and bronchoscopic samples are the most commonly utilized and trustworthy biomarkers [116,117]. Different biological specimens, including blood, urine, sputum, saliva, and exhaled air, are used to extract and quantify biomarkers [10]. Biomarkers based on genetic materials, such as DNA, miRNA, and others, are primarily detected in blood, bronchoscopic samples, sputum, and nasal epithelium, whereas volatile organic compounds (VOCs) are mostly found in exhaled breath. Table 3 lists the various widely used biomarkers.

Various sampling methodologies for biomarkers detection are [10]

(1) Liquid biopsy.
(2) Sputum cytology (SC).
(3) Breath analysis.

4.1.1 Liquid biopsy

Oncologists and basic researchers are interested in liquid biopsy, a less invasive technique for the early diagnosis of LC. The primary goal of this approach is to examine

Table 3: Various widely used biomarkers [10]

Biomarkers	Details about the biomarker	Reference
AAbs	The activity of serum AAbs using tumor antigens was studied in this investigation. ELISA results showed that serum anti-cyclin B1 and anti-HCC1 levels increased in the first three stages of LC while anti-p53 levels increased significantly in stage I only. Anti-Survivin-Aabs increased in the second and third phases of LC. This study has shown to have a sensitivity of 65%	[118]
Complement fragments	Complement factors C5a, H, C4d, and other biomarkers have been recommended as biomarkers in LC by various research studies. Most NSCLCs exhibited complement factor H, which enhanced C5a release and caused cytotoxicity	[119,120]
miRNA, ctDNA, and hypermethylated DNA	According to a recent study, these biomarkers are vital for detecting LC with a sensitivity >60–80%	[121]
Proteins	Protein profiling using LB has a key role in identifying LC, according to foremost research. The study created a panel with 71% sensitivity and 88% specificity for diagnosing NSCLC using three blood proteins: cancer antigen 125, CEA, and cytokeratin with AAb	[122]

circulating tumor cells (CTCs) and/or circulating tumor DNA (ct DNA) [71]. In addition to the diagnosis of LC, a liquid biopsy may now be used to forecast customized prognosis based on genetic changes and monitor diseases based on characteristic molecular markers, making it more practical in clinical practice than before [123]. LC has traditionally been diagnosed histopathologically using information available from tissue samples. A tissue biopsy can also assist oncologists in determining the stage of LC and, as a result, therapeutic options. Tissue biopsy, on the other hand, has the following drawbacks: (i) it is an intrusive process, (ii) it is an inaccurate diagnostic method in terms of tumor heterogeneity and distant metastasis, and (iii) it is not reproducible [71]. These features of tissue samples may necessitate additional examinations of patients. Liquid biopsy, on the other hand, has been shown to be a feasible proxy for the noninvasive evaluation of tumor-specific biomarkers in the diagnosis of LC. As a result, it has the potential to be applied for various therapeutic and research applications [124]. Several liquid biopsies were investigated in blood, like circulating nucleic acid, CTCs, *etc*., to address the limitations associated with early diagnosis of LC [124]. One of the most intriguing and increasing disciplines in diagnosing LC is the capacity to examine the genetic profile of cancer cells by a noninvasive sampling of blood or other bodily fluids [125]. Further details on each of these biomarkers can be obtained elsewhere [123–125].

4.1.1.1 MicroRNAs (miRNAs)

Both healthy individuals and LC patients have circulating miRNAs in their blood. MiRNA could be utilized as a diagnostic biomarker because of its stability [69]. MiRNAs participate in a variety of bioactivities by controlling gene expression and are refactored by a number of important components. Furthermore, particular deregulation of miRNAs has been related to LC, making them a good candidate for molecular diagnostics. Endogenous miRNAs are also resistant to nucleases and durable under severe temperature changes. As a result, miRNAs can be accurately measured and replicated *via* RT-PCR for LC detection [126]. Microvesicles (exosomes) produced by platelets or phagocytic mononuclear cells may carry miRNA into the circulation. Exosomes emanating from cancer cells have also been discovered [127], suggesting the prospect of distant signaling and niche preparation for metastatic dissemination, which is a developing study topic [128]. The relationship between plasma miRNA expression and LC has been studied by various researchers. Wozniak *et al.* [129] examined circulating plasma miRNAs in stage I–IIIA LC with suitable controls to find a 24-miRNA panel with differential expression. Another research looked at two particular miRNAs, miR944 and miR3662, in 85 healthy controls and 90 patients, and observed that both miRNAs were overexpressed by more than fourfold in NSCLC patients compared to healthy controls. Among squamous cell carcinomas and adenocarcinomas, there was no significant change observed in the expression of these two miRNAs [130]. Shen *et al.* [131] discovered four miRNAs (miR-21, miR-126, miR-210, and miR-486-5p) in plasma that had sensitivity and specificity of 86 and 97%, respectively, in NSCLC patients from controls. Surprisingly, this panel exhibited a greater sensitivity (91%) for adenocarcinomas compared to squamous cell carcinomas (82%). The same researchers examined the expression of plasma miRNA in benign and malignant solitary pulmonary nodules (SPNs). In malignant SPNs, miR-21 and 210 were increased, whereas miR-486-5p was downregulated compared to benign SPNs. As a result, the authors were able to construct a model that had sensitivity and specificity of 75 and 85%, respectively, for identifying malignancy in CT-detected SPNs [132]. MiRNA analysis has been investigated in such a way so that it can increase the efficacy of LC screening programs. Boeri *et al.* [133] examined miRNA expression in plasma from patients in an LDCT lung screening trial [134] to find out the differential expression of miRNAs before and after the onset of LC. A panel of 15 miRNAs was found for detection prior to diagnosis, and a panel of 13 miRNAs was identified for diagnosis (with considerable overlap to the first 15). These were tested on plasma samples from the MILD research [135] and found to be accurate. Prior to diagnosis, sensitivity, and specificity of 80 and 90%, respectively, were achieved, whereas upon diagnosis, sensitivity and specificity 75 and 100%, respectively, were acquired. Furthermore, in the validation cohort, a panel of nine miRNAs was able to predict poor prognosis with sensitivity and specificity of 80 and 100%, respectively [133]. These miRNAs were combined into a panel of 24, which was then used to create a miRNA signature classifier, which was used to categorize patients into low, moderate, and high-risk groups. This technique was blindly applied to a larger patient population from the MILD trial and found to have sensitivity and specificity of 87 and 81%, respectively. It decreased the false-positive rate by fivefold when coupled with LDCT [136]. Furthermore, in terms of 5-year survival, there was a statistically significant shift from low risk to high risk. Although the use of circulating miRNAs appears to be promising for early identification of NSCLC, well-designed, independent, and high-powered validation studies are the need of the hour to validate its further applications.

Xing *et al.* [137] discovered that miRNA 21, miRNA 31, and miRNA 210 detected in the sputum of the patient are

excellent biomarkers for early diagnosis of LC and malignant SPN in a recent clinical trial. The test's overall specificity was found to be between 80 and 86%, while its sensitivity was found to be between 82 and 88%. The use of SC (Section 4.1.2) in combination with LDCT can enhance the overall diagnostic sensitivity; however, biomarker validation is yet to be established [137]. Su *et al.* [138] have observed that using hypermethylated genes as a biomarker in conjunction with miRNA enhances the specificity of NSCLC diagnosis. In a clinical investigation of miRNA with three genes (RASSF1A, PRDM14, and 3OST2), it was discovered that combining miRNA 31 and miRNA 210 with the genes RASSF1A and 3OST2 enhanced specificity and sensitivity (by 90%) in the diagnosis of NSCLC [138]. Another fascinating work focused on the identification of noncoding RNA species, such as short nucleolar RNA (snoRNA), which is known to have a role in carcinogenesis. Sputum snoRD78 and snoRD66 are effective biomarkers in the identification of LC, according to clinical research [139], with a sensitivity and specificity of 74 and 84%, respectively.

4.1.1.2 ctDNA

DNA is assumed to enter the plasma either passively or actively [69]. In cancer patients, a part of this cell-free DNA comes from the tumor, forming the so-called "circulating tumor DNA" (ctDNA) fraction [140]. In a research study, frequent mutations were found to establish a library for identifying mutations linked with NSCLC, demonstrating the usefulness of ctDNA in LC. In a validation cohort of healthy controls and NSCLC patients, the sensitivity of 85% and specificity of 96%, respectively, were achieved. There was also a relationship between tumor volume and the amount of ctDNA in patients over time, suggesting that ctDNA may be used to track therapy response. The presence of ctDNA was found in all late-stage NSCLC patients, but only in 50% of early-stage instances [141]. Blood samples were collected from healthy adults at risk of cancer due to occupational/tobacco exposure as part of the GENAIR project, a multinational European prospective study. TP53 and Kirsten's rat sarcoma viral oncogene homolog (KRAS) mutations were detected on average 20 months and 14 months before cancer diagnosis, but only in 4.6 and 1.5% of patients, respectively. Furthermore, TP53 and KRAS mutations were found in 3 and 0.9% of controls, respectively, who did not develop cancer during a 5-year follow-up period [142]. In order to establish an early detection assay, one study looked at TP53 mutations in early- and late-stage SCLC and compared them to controls to see how specific this method was. TP53 mutations were found in 35% of early-stage tumors and 54% of late-stage tumors, as well as 11% of matched controls [143]. Quantifying the human telomerase (hTERT) gene has been used to determine the total quantity of circulating DNA. Patients with NSCLC exhibited substantially greater circulating levels than age/sex/smoking matched controls using this method [144]. The follow-up research looked at total circulating DNA in a group of individuals with a long smoking history who were part of an LDCT observational trial. Although greater circulating DNA at diagnosis was indicative of a poorer outcome, there was no link between total quantities of circulating DNA at baseline and risk of future malignancy [145]. Furthermore, total circulating DNA measurement is not specific to NSCLC; for example, higher levels of circulating DNA have been reported in idiopathic pulmonary fibrosis [146]. The present therapeutic usefulness of ctDNA rests in the customization of ctDNA assays based on biopsy-derived genomic landscapes, as well as the subsequent monitoring of patient response and emergent treatment resistance, as well as tumor development [147]. Common LC mutations, such as p53, can be utilized in screening, although they are also present in individuals with a smoking history who do not have LC, which leads to confusing specificity [148]. Furthermore, evidence for widespread genetic mosaicism in healthy tissue is accumulating, including the presence of mutations in genes known to have a role in cancer [149]. While candidate gene analysis based on droplet digital PCR has greater sensitivity, as the sensitivity of next-generation sequencing (NGS) improves, a larger panel of genetic alterations may be more informative on tumor occurrence.

4.1.1.3 CTCs

As aggressive malignancies progress, cell subpopulations change morphologies and become motile, infiltrating surrounding tissue and obtaining access to the bloodstream through a variety of processes such as epithelial-to-mesenchymal transition [150], cell cooperation [151], and vasculogenic mimicry [152]. These so-called CTCs are heterogeneous and are thought to include the fraction of cells responsible for distant metastasis formation [153]. CTCs generated from SCLC patients have been found to be tumorigenic in mice, generating explants that perfectly recapitulate the response to therapy seen in the original patients [154], lending validity to this perspective in the LC area. CTCs may be detected using a variety of techniques [155] and they are increasingly being used as a qualitative and quantitative indicator of cancer burden. CTCs counted

(using the Cell-Search platform) and captured *via* epithelial cell adhesion molecule (EpCAM) expression are predictive in metastatic breast [156], prostate [157], and colorectal malignancies [158]. CTCs identified by Cell-Search are very common in SCLC; in one research, 85% of patients had detectable CTCs, and having more than 50 CTCs in 7.5 mL of blood was an independent predictive biomarker [159]. Cell-Search CTCs were identified in only 23% of patients with stage III/IV NSCLC, although being prognostic (at higher than 5 CTCs in 7.5 mL of blood) in NSCLC, compared to a size-based filtering technique that generated detectable CTCs in 80% of patients in the same cohort [160]. Despite this, research on NSCLC was able to improve the sensitivity of Cell-Search in NSCLC by quantifying CTCs from the pulmonary veins at the time of surgery in stage I–IIIA NSCLC, where larger quantities of CTCs were associated with shorter patient survival [161]. These findings suggest that CTCs shed from early-stage NSCLCs may help with LC early detection and, as a result, patient survival. The use of CTCs in early-stage diagnosis has piqued attention. Cell-Search was utilized to quantify CTCs in single-center research of patients sent to a thoracic center with either a histological diagnosis of LC (SCLC and NSCLC) or high suspicion; however, they were only present in 31% of patients who were later diagnosed with LC. The quantity of CTCs did, however, correspond with later stages of illness, which is consistent with earlier research [162]. Using a variety of CTC detection techniques is likely to pay off in terms of early detection. Isolation by size of epithelial tumor cells (ISET) identified CTCs in 50% of NSCLC patients before radical therapy, compared to 39% with Cell-Search. In 69% of cases, combining the two methods resulted in detection [163]. Only five individuals with identifiable CTCs developed LC during a 5-year follow-up period, according to the greatest evidence so far for CTC usefulness in earlier identification of LC using ISET alone in a cohort of 168 COPD patients. The rest of the patients lacking CTCs, on the other hand, were LC-free at the conclusion of the follow-up period [164]. A ligand PCR technique was employed in another investigation to quantify CTCs. Following immunological depletion of erythrocytes and leukocytes, cells were tagged with a folate receptor (FOLR1) ligand coupled to an oligonucleotide, allowing real-time PCR (RT-PCR) measurement. This method detected CTCs in 8 of 10 stage I/II NSCLC patients examined, with an overall sensitivity of 82% and specificity of 93% for stage I–IV NSCLC diagnosis compared to controls [165]. The relatively uncommon occurrence of CTCs in even advanced late-stage patients in comparison to the overwhelming amount of blood cells in the sample is a technical obstacle for CTC detection. Marker-dependent capture is hampered by CTC heterogeneity, and not all CTCs are bigger than blood cells, creating problems for size-based approaches. Furthermore, every CTC enrichment procedure results in cell loss. The high-definition single-cell analysis platform, for example, is better suited to early detection since all cells in the sample are examined using a flexible panel of markers, and cells may be photographed and physically chosen for single-cell genetic analysis to establish tumor origin [166]. The value of CTC analysis for early detection is yet to be fully explored, as has the question of whether survival time will be extended after CTCs are detected. Patients benefit from molecular profiling of "early" CTCs since it allows for earlier intervention and customized treatment.

4.1.2 SC

Exfoliated cells of the bronchial and pulmonary epithelium make up sputum, a noninvasively accessible type of bodily fluid [10]. SC is the process of generating, collecting, and examining secretions from the lungs under a microscope for abnormal cells. Advanced SC [167] entails the identification of particular LC biomarkers in sputum with enhanced sensitivity and accuracy. Exfoliated cells from the larynx, pharynx, bronchi, and buccal cavity are found in the sputum. Induction and sputum collection might be difficult since the quality and quantity of sputum are typically inadequate for testing. Sputum is collected spontaneously or artificially utilizing procedures such as hypertonic saline aerosol preparations, salbutamol (bronchodilator), and/or a physical approach of vigorous breathing aided by a qualified professional. The delivery of hypertonic saline aerosol spray is the preferred method due to higher patient compliance, whereas the manual technique necessitates expert help [168]. When the patient is unable to generate significant amounts of sputum, additional or repeated inductions may be used to improve accuracy [169]. This method is advantageous because pooled sputum samples produce better results than spontaneously inspected samples [170]. SC accuracy is often determined by the examiner's expertise, as well as the size and position of the LC lesion. Due to these factors, further testing CT or bronchoscopy is required to establish the presence of a tumor. As a result, SC in combination with techniques has emerged as a new diagnostic technique in the early identification of LC.

4.1.3 Breath analysis

Various exogenous and endogenous volatile biomarkers have been investigated for the detection of LC in recent

years [10]. The majority of exhaled breath indicators are exogenous in origin and have been linked to cigarette use. A variety of chemical and inorganic substances collected at the respiratory tract's periphery enhance exhaled breath (EB). The presence of intermediate and end products of metabolism in these volatile mixtures indicates cancer-related bioactivities. Any aberrant pathogenic activity can be revealed by EB analysis. Due to the simplicity with which data may be captured from EB, EB analysis is becoming a more intriguing topic for gas sensing technologies. The methodological problems associated with EB collection and analyses are highlighted in the recent research by the European Respiratory Society Task Force (ERS TF) [171]. Breath testing, according to the TF, should look at three types of chemicals: EB nitric oxide, VOCs, and EB condensate (EBC). Although the procedures for collecting and analyzing nitric oxide and EBC are well-documented, these criteria for VOCs are not. Several variables, including sample amount, collection duration, and so on, should be controlled during the collection and analysis of EB, according to the recommendations of the ERS Task Force. To maintain the stability of the biological markers contained in EB, the period between collection and investigation must be as brief as feasible. Also, before and after processing, the pH of EBC should be verified using pH measurements taken at calibrated CO_2 concentrations (5.33 kPa). Other factors such as EBC volume, dilution factor, presence of nonvolatile components, and process repeatability must also be standardized [171].

In the future, breath analysis would be used as a supplementary diagnostic tool, alongside traditional radioimaging techniques [172]. VOCs in exhaled air and their condensate can be measured to detect LC in confirmed instances of NSCLC, according to a recent study. The findings show that VOCs such as hexane, heptane, pentane, and others are strong markers of NSCLC and assist to distinguish them from healthy individuals, with an AUC of 85–90% in smokers [173]. Furthermore, LC disrupts current biological processes and promotes the onset of oxidative stress. This process results in the production of VOCs, which are metabolic products. According to recent clinical research, carbonyl molecules can be utilized to diagnose LC, with overall accuracy ranging from 80 to 100% [174]. Furthermore, a groundbreaking study revealed 2-butanone and 1-propanol as the best and most promising VOC biomarkers for LC detection [175]. In addition, a recent research study looked into methods such as enzyme-linked immunoassay, antibody-based microarray, and fluorescent bead-based test for detecting VOCs in EB with sensitivity ranging from 50 to 70%. EB analysis also has the advantages of reproducible assessments, noninvasiveness, and the creation of customized therapy. In addition, a significant study looked at the effect of expiration flow rate, anatomical dead space, and breath-hold on the efficiency of the electronic nose in detecting LC. This study discovered that flow rates, breath-hold, and dead space had a substantial influence on breath prints created by the electronic nose, which detects VOCs in EB. The results showed that there was a substantial difference between the breath prints of LC patients and healthy volunteers at a flow rate of 50 mL/s, with an accuracy of 72%, and at a higher flow rate of 75 mL/s, with an accuracy of 78%. Similarly, with a breath-hold of 10 s and 70% accuracy, the discriminating power was substantial. According to the findings, electronic nasal standardization is necessary for obtaining precise analyte values. Furthermore, additional equipment such as GC-MS should be used to increase VOC specificity and discrimination [176].

4.2 Microfluidic chip

The microfluidic chip is a well-organized, competent, efficient, rapid, and accurate diagnostic tool for LC patients. The manipulation of fluids on a microscopic scale is possible by using a microfluidic chip to control relevant parameters of cell culture [9]. This provides a better simulation of the tumor microenvironment *in vivo*. More specifically, it is possible to operate the cells precisely using the microscopic structure of a microfluidic chip and it is easy to conduct high-yield output analysis by the use of multiplexing microstructures [9]. The microfluidic control is beneficial to impersonate the internal fluidic environment, and its specific material characteristics can better mimic the microenvironment of tumor tissues. In precision medicine, the application of microfluidic chips can become a powerful assisting equipment to be realized in diagnostic forms [177], especially in the tumor organoid culture field single-cell sequencing, cancer biomarkers detection, and nanoparticles synthesis. In view of these functions, the combination of the microfluidic chip with downstream analysis can better identify cancer progression by studying its cellular, molecular, and biophysical properties [178].

Microfluidic devices have a remarkable prospect for development in the field of cancer metastasis because of their customizable properties, and they can meet the demands of various research works worldwide. These chips have rapid and high throughput, require a small volume of sample, have lower LOD, are flexible, are of small footprint, and are suitable for longitudinal collection. In the organoid culture field, microfluidic devices

are used to culture two or more organoids to mimic cancer progression and can be applied to different types of cells. The separation of different organoids is conducted by the use of some definite biomaterials, like polydimethylsiloxane (PDMS), while the channels and controllable fluids are used to connect them with each other. The design and construction of a multiorgan microfluidic chip have been reported by Xu *et al.* [179] to mimic LC metastasis to different body organs such as the brain, bone, and liver. For this purpose, the organoids were divided into different chambers with an upper chamber for lung organoids and a lower for the other three organoids. Each chamber was seeded with various cell types to culture different organoids and the side channels were used to link each organoid. For simulation of blood circulation, the culture medium flowed through microvascular channels, and simultaneously a circulating vacuum was connected to mimic the physiological breathing as shown in Figure 5(a) [179]. This system helps effectively in exploring the complex process of underlying LC metastasis mechanisms. As depicted in Figure 5(b), another research reveals a microfluidic bone chip (BC) to explore metastasis of breast cancer to bone marrow.

Based on the simultaneous growth dialysis principle, there are two areas in the space of BC one for osteoblastic tissue growth and the other for culture medium flow [180]. This cancer model presented a natural bone microenvironment that allows the formation of an extraordinary thick layer devoid of artificial scaffolds by biomineralization of osteoblastic tissues or *in vivo* growth step. Moreover, researchers also developed osteoblastic tissue in the BC for co-culturing the metastatic human breast cancer cells and perceived various noteworthy characteristics of bone metastasis in breast cancer. Thus, the microfluidic BC has the potential to become powerful equipment in the *in vitro* study of bone cancer metastasis.

4.3 Biosensors

The functionalized MNP surfaces offer linkage groups to permit binding events with the complementary biomolecules. As discussed in Section 2.2.1, different strategies for bioconjugation include [8]:

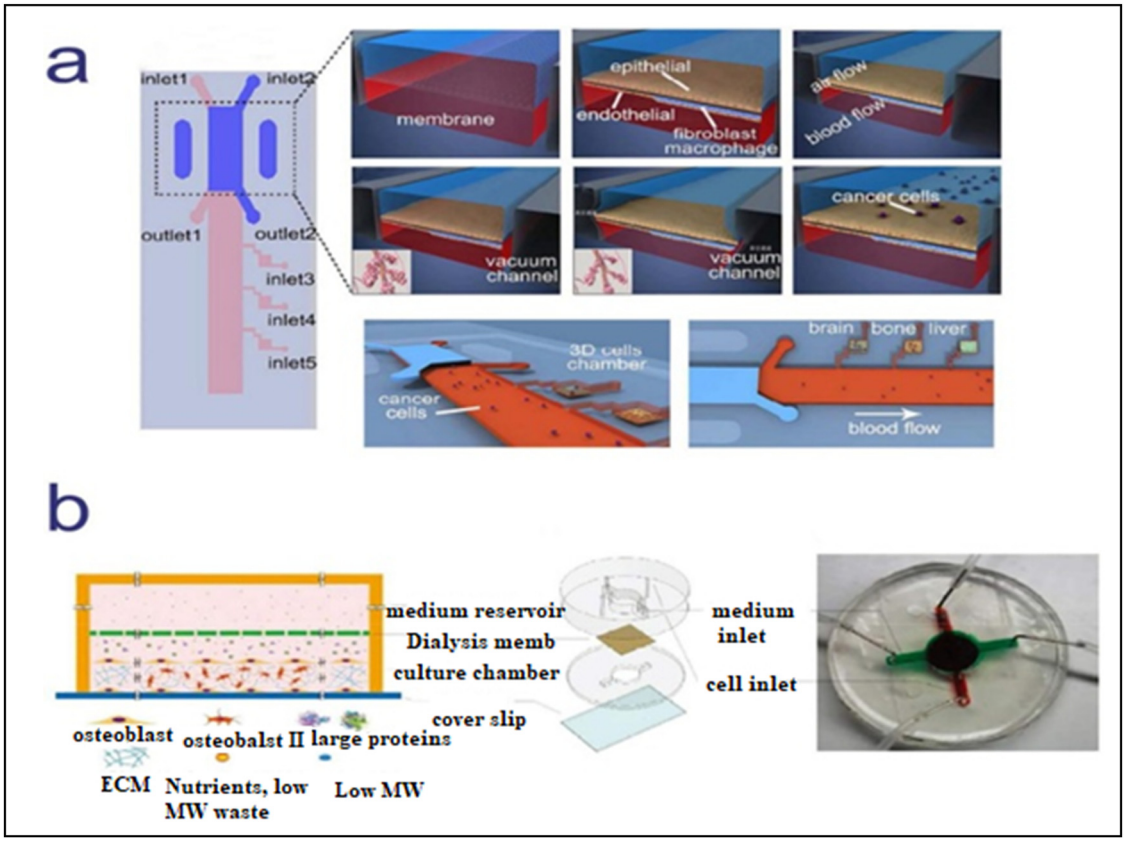

Figure 5: Cancer models based on microfluidic chips; (a) a multiorgan microfluidic chip that mimics LC metastasis in the brain, liver, and bone; (b) cancer model to study breast cancer metastasized to bone marrow. Reprinted from ref. [9] by Creative Commons License.

(1) Physical interactions (hydrophilic–hydrophobic, affinity interactions, and electrostatic interactions).
(2) Chemical interactions (covalent bonds).

These interactions make immobilization on MNPs or transducers easy and simple. Specific interactions between protein and their recognition elements have shown their utilization in the development and designing of biosensors. There are different sensing/biosensing methods to determine the level of cancer biomarkers in blood, plasma, or diseased tissues. Some of them are listed below:
(1) Electrophoresis.
(2) Optical methods (fluorescence, electrochemiluminescence, colorimetric assay, SPR, SERS, *etc.*) (Table 4) [181–183].
(3) Immunological methods (ELISA, polymerase chain reaction (PCR), *etc.*) [165].
(4) Microcantilevers.
(5) Electrochemical assay, electro-conductive, piezoelectric, and amperometric biosensors [184–186].

There are different labeling approaches to outline biosensing events depending on the method (electroactive molecules, fluorescent labels, nano/microparticles, enzymes, *etc.*). The following are the two primary techniques for integrating MNPs into the biosensor design [8]:
(1) **Direct labeling**: In this approach, MNPs are immobilized at the transducing element *via* an affinity recognition reaction such as MNPs functionalized with single-stranded DNA as a capture probe is used to modify the sensor surface, and the hybridization reaction occurs when complementary oligonucleotides come into contact with the sensor, resulting in a physical/chemical response.
(2) **Indirect labeling**: The ELISA technique is used in this procedure such as primary antibodies that are complementary to the targeted protein are immobilized on the sensing surface, followed by an affinity reaction with a biomarker-containing solution. Later on, secondary biotin-labeled antibodies are added to the system, allowing for an affinity interaction between streptavidin-labeled MNPs and the sensor surface.

Microelectronics' contribution to sensor technology is helpful in the creation of devices that can detect LC biomarkers. Several biosensors, including optical and electrical conductance sensors, have been proven for the diagnosis of cancer-associated proteins, in recent years [10]. Simultaneously, the importance of investigating volatile metabolites that might be directly examined from the breath to identify LC is increasing [10]. Capuano et al. [187] conducted a survey of current state-of-the-art volatile chemical sensors and biosensors. CYFRA21-1 and NSE are two of the most reliable LC indicators [70]. These indicators are well-known for distinguishing between the two most common types of LC: NSCLC and SCLC. In serum having standardized immunosorbent tests, the identification of these compounds can be detected. However, such methods need the tagging of the target molecule in order to identify it. The fast label-free technique of detection can identify immunoselective interactions. Cheng *et al.* [188] developed a field-effect transistor biosensor in which the human antigen CFYFRA21-1 and NSE were covalently linked on the sensitive surface. Because of the lack of a labeling technique and the great sensitivity of the device, these markers can only be detected at concentrations of around 1 ng/mL. In a study, the development of an ultrasensitive aptamer for the diagnosis of A549 LC in human blood serum with high sensitivity

Table 4: Optical biosensors in LC detection [10]

Sensor	Biomarker	Details	Reference
SPR-based sensor	Cytokeratin-based CK-7 biomarkers	For the detection of cytokeratin required in LC, an optical biosensor based on the lab-on-chip idea has been developed. SPR-based sensors have been designed for the detection of CK7 biomarkers with high sensitivity (0.4 nM)	[181]
SPR-based sensor on the chip	CK19 cells	For the identification of CK19 LC cells in plasma, a graphene oxide-based SPR sensor-on-chip has been designed. It has shown a detection limit of 0.001–100 pg/mL, which makes it extremely sensitive. Selectivity, specificity, precision, and repeatability are all desirable properties of this new sensor	[182]
QDs-based sensors	miRNA	A fluorescent strip biosensor based on quantum dots has been developed to detect miRNA with ultrasensitivity. The sensor is extremely sensitive and will help to come up with enzyme-free detection in point-of-care diagnostics in the future	[183]

(8 cells/mL) was reported by Wu *et al.* [189]. A new aptasensor for early detection and monitoring of LC was developed using cyanine dye and an S6 quadruplex aptamer with increased fluorescence. Furthermore, a recent study by Zhao *et al.* [190] reported aptamer cocktails for the CTC detection in LC by the use of microfluidic assay and the detection process employed aptamers. Aptamers are defined as highly specific, selective, sensitive, and precise techniques for LC monitoring with a scope for expansion in the field of future sensing. With the rapid application of biosensors in diagnostics and monitoring systems, IONPs/SPION- based biosensors are under investigation for their prospective in LC diagnostics. On the same lines, Kumar *et al.* [191] reported an electrochemical paper-based sensor using IONPs, and Yu *et al.* [192,193] designed an aptamer conjugated with thermally cross-linked SPIONs showing promising leads in terms of LC detection.

4.4 Nanotheranostics

Theranostics is a new field of biomedicine and bioengineering that specializes in disease diagnosis and therapy, particularly cancer [10]. Nanoparticles based on theranostics are becoming a more advanced platform for overcoming the limits of a traditional cancer diagnosis. For the real-time study of illnesses like cancer, theranostics combines several diagnostic imaging techniques with theranostic monomolecular agents. Multifunctional carbon nanodots for gene delivery in the treatment and diagnosis of LC were developed in recent research [194]. The photoluminescence characteristics of these nanodots are used to deliver siRNA in the treatment of NSCLC. These nanodots are injected into the body and deposit at the tumor site, emitting blue light fluorescence between 300 and 400 nm, and the siRNA contained in them induces tumor regression by apoptosis. This new theranostics nanoagent has shown promise in the detection and therapy of NSCLC [194]. Another intriguing study focused on the theranostic implication of boron neutron capture treatment and its effectiveness in LC [195]. The research involves the creation of boron/gadolinium-LDL adducts with detectable radioactivity and efficient cytotoxicity against lung tumors utilizing MRI. This enhancing approach may also be used to assess tumors with a diameter of less than 0.2 mm [195]. Researchers also synthesized a hyaluronic acid-based nanogel for PTT for LC diagnostics with continuous doxorubicin release. pH-responsive hyaluronic acid, photoresponsive graphene, and doxorubicin were used for the preparation of the nanogel. Graphene accumulates in tumor cells when this conjugate is injected into the body, and irradiation causes doxorubicin to be released sequentially from the conjugation. This is a very sensitive method of detecting and treating LC.

Another technique for early detection of LC involves the functionalization of MNPs collectively with antibodies and chemotherapeutic drugs [196]. Antibodies are highly specific for a particular antigen; thus, they will help in the targeted delivery of the drug. Photodynamic treatment, PTT, and magnetically induced hyperthermia have all been used with MNPs as a nanotheranostics technique for the diagnosis of LC [8]. These methods are used in the branch of medicine called oncology. The combined effect, on the other hand, typically confirms the most important diagnostic outcomes. This has been ascribed to MNPs' modular architecture, which allows them to perform many functions. Figure 6(a) shows an example of how MRI was utilized to diagnose cancer early. Chemotherapeutic therapy combined with MRI resulted in better results [8]. The protocol used in the synthesis process regulates and changes the final characteristics of MNPs. The application of an external magnetic field inhibited MNPs' clustering, and this magnetization was lost as soon as the field was withdrawn, preventing MNPs' aggregation [8]. As discussed earlier, some MNPs have a magnetocaloric effect, in which the temperature of the MNPs changes in the presence of an external magnetic field. The magnetocaloric effect, along with MNPs' high surface-to-volume ratio, allowed for efficient heat exchange with the environment. This enabled the development of the cancer treatment method known as "hyperthermia." Figure 6(b) shows how MNPs' unique features are completely subdued in tissue labeling and targeted drug delivery locations. The drugs were delivered to the precise target cell by placing the magnetic field outside of the anatomical structures and using an *in vivo* transportation approach [8]. MNPs absorb heat generated by electromagnetic waves in alternating cycles, making this magnetic material suitable for tumor detection in general. MNPs' small size has a significant influence. The role of MNPs in LC diagnosis is linked to their use as a distinguishing agent in MRI and as a heating intermediary in hyperthermia (Figure 6(c)) [8]. Figure 6(d and e) further depicts the unique functions and properties of MNPs as a platform for antibody immobilization in the design of biosensors. Affinity ligands such as aptamers, hEGF, lectin, and folic acid have been associated with the surface of MNPs in order to guide them into tumors. As demonstrated in Figure 6(f), this promoted the accumulation of MNPs in a specific cell or tissue site [8,86–88]. The use of these strategies in conjunction with guided medication administration

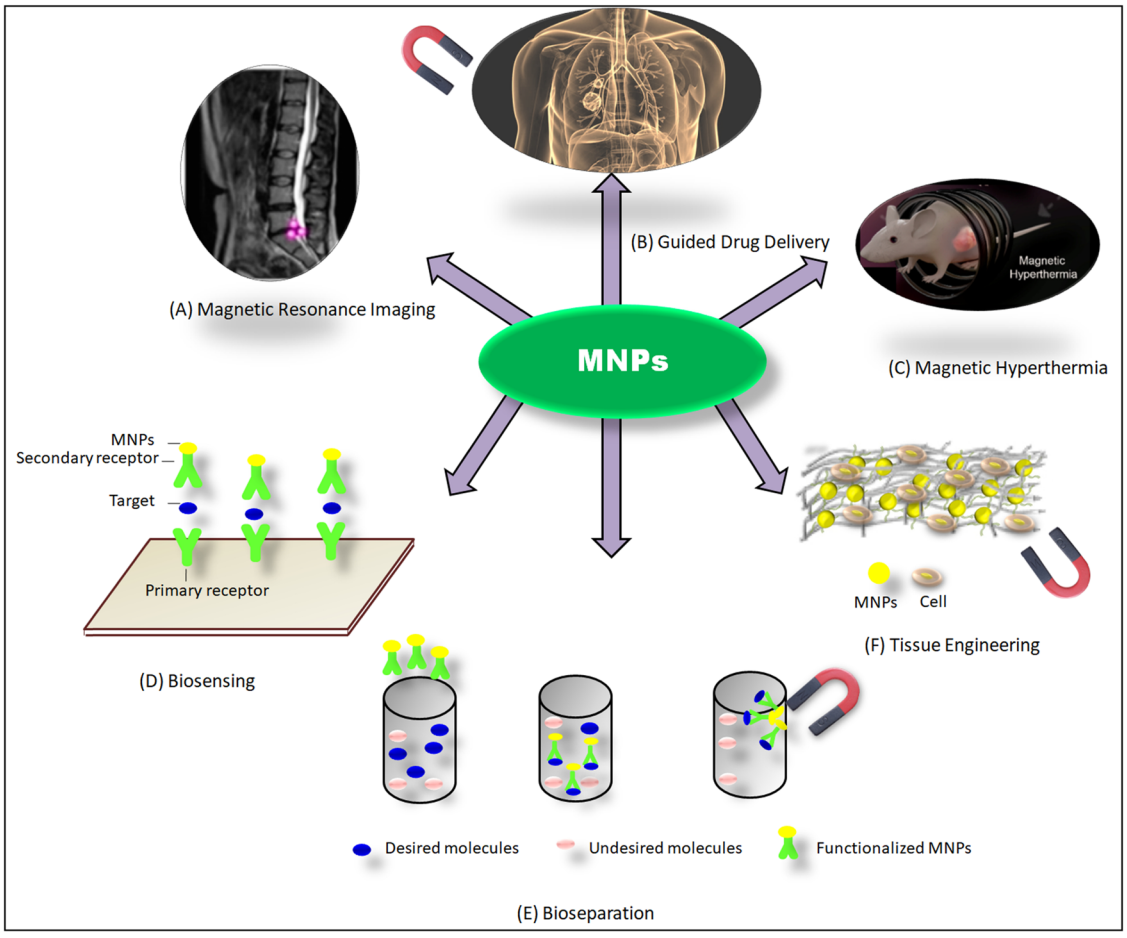

Figure 6: Schematic presentation of various applications of MNPs: (a) MRI, (b) drug delivery, (c) magnetic hyperthermia, (d) as biosensors, (e) bioseparation, and (f) tissue engineering in biomedicine. Reprinted from ref. [8] by Creative Commons License.

and magnetic hyperthermia has resulted in a synergetic effect in the accurate identification of LC.

Wang *et al.* [196] demonstrated successful coupling of synthesized MNPs with pan cytokeratin antibody, abbreviated as pan-ck Ab (Figure 7), as well as two additional types of prepared QDs conjugated with Lunx and SPC-A-1 antibodies. The simultaneous usage of QDs with double-labeled antibodies was applied for detecting the CTCs of NSCLC patients assembled by MNPs combined with pan-ck (MNP-pan-ck). MNPs and QDs were used to successfully construct a unique and creative approach for evaluating micrometastases of LC in peripheral blood. With its separation and visibility, the coupling of MNPs with QDs allows for the simple identification of specific cancer cells. Excess fluorescence multilabeling in combination with functionalized MNPs might be used to produce images with multicolor fluorescent molecules and magnetic variations. The conjugation of specific CTCs or CTCs [197] occurs when the anti-epithelial cell adhesion molecule antibody (EpCAM Abs) is immobilized. It depicts a schematic of micrometastasis detection in LC using the combined influence of MNPs and QDs [196]. It was found that QDs with double-labeled antibodies successfully identified LC cells A549 and SPC-A-1. As a result, a total of 32 cases of NSCLC were discovered. Twenty-six patients had improved CTCs, and 21 patients were effectively identified by QDs. As a result, a novel approach was developed in which CTCs were collected using MNP-pan-ck, and CTCs from NSCLC patients were identified using QDs with double-labeled antibodies.

4.5 AI

Many aspects of the healthcare industry have been profoundly affected by AI and ML [14]. Technology advancements have paved the path for cost- and time-effective analysis of large datasets. AI is proving to be beneficial in clinical oncology and research [198]. NGS systems were introduced to meet these needs and they have changed the future of precision oncology [199]. NGS has numerous

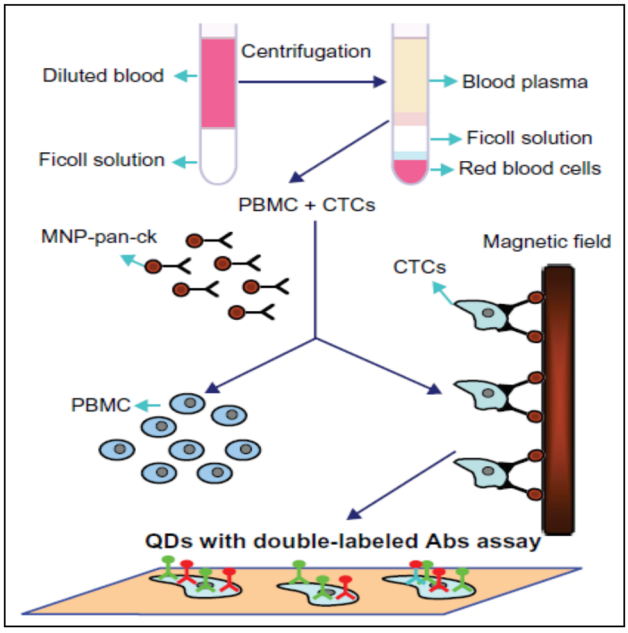

Figure 7: Schematic presentation of recognition and separation of tumor cells using MNP-coupled pan cytokeratin antibody and QDs with double-labeled antibody [196] (PBMC: peripheral blood mononuclear cells). Reprinted ref. [196] under Creative Common License.

clinical uses, including risk prediction, early disease detection, diagnosis by sequencing and medical imaging, accurate prognosis, biomarker identification, and therapeutic target identification for new drug development. NGS creates enormous datasets, which necessitate the use of specialist bioinformatics tools to evaluate the data that is therapeutically useful. Cancer diagnosis and prognosis prediction are improved using NGS and high-resolution medical imaging, thanks to these AI applications. Regardless of technological advancements, AI's pattern recognition and sophisticated algorithm skills may be used to get important clinical information, reducing diagnostic and treatment mistakes [200]. In cancer, ML is a useful technology with many applications in precision medicine. Complex neural networks can predict disease and treatment results by generating diagnostic pictures and genetic analysis data [200,201]. Deep learning algorithms are employed in the healthcare sector for the curation of vast amounts of data and the creation of improved data-driven diagnostics. Biomarkers are found in medical imaging and can be used to screen patients for cancer. Image analysis entails identifying the image of interest as well as significant sections of the image. Data from datasets and the results of patient screening can be utilized to detect malignant tumors automatically. Using AI algorithms, we can thus customize our treatment options in the event of a cancer diagnosis [14,198]. Deep learning is the most often used AI technique in radiomics, a field of computers that extract diagnostic images to discover malignant tumors that are not visible to the naked eye. The combined efforts of radiomics and deep learning will improve diagnostic picture analysis accuracy [201]. When AI and ML are used in healthcare, they have the potential to transform illness management and deliver effective medical care. AI research has progressed to the point where it can make decisions in a human-like fashion (Figure 8). AI can improve the sensitivity, repeatability, and accuracy of tumor detection not just through automated segmentation but also through the rapid increase in computing speed and by enhancing AI algorithms. It is conceivable that a separate segmentation analysis of suspicious images will become obsolete. Consequently, AI systems can evaluate image data from the whole body.

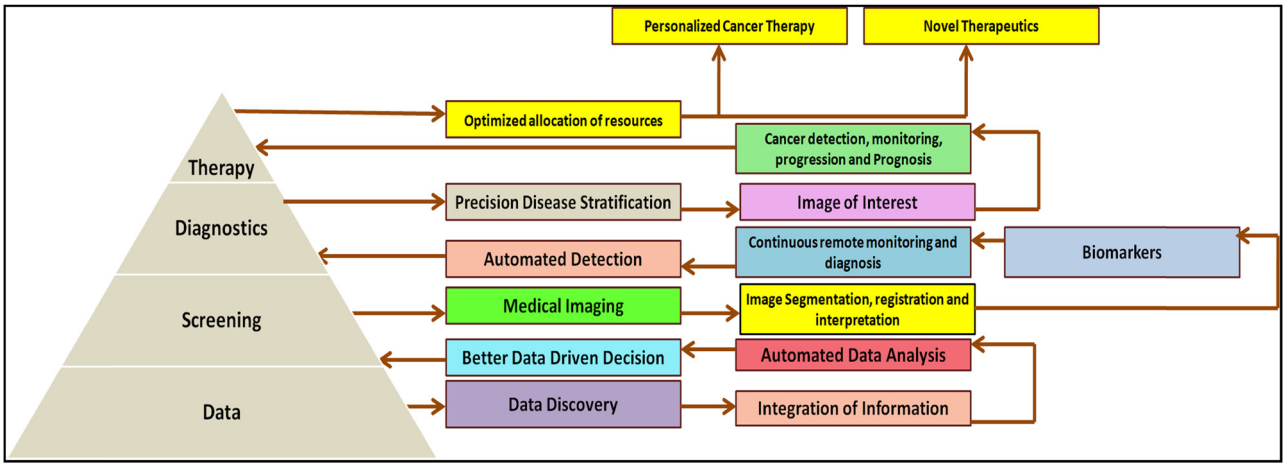

Figure 8: Application of AI in cancer imaging to create better data-driven diagnoses using deep learning algorithms.

In this sense, a full-body approach will allow a more detailed study of the organs' properties that can be modified by pathological processes but are invisible to human sight. This means that these algorithms could be used in various aspects of early LC diagnosis, such as information from serological studies and tissue biomarkers.

In the search for surrogate markers of LC, researchers have looked at biomarkers derived from body fluids and tissues such as whole blood, plasma, bronchial lavage, urine, sputum, and biopsy specimens. Studies have shown that CTCs, AAbs, miRNAs, EB biomarkers, and blood proteomic profiling are promising molecular candidates for the early detection of LC [69–71]. Finally, high-throughput technologies such as epigenomics, transcriptomics, and metabolomics are also being explored as potential indicators of early LC [202]. The combination of numerous "omics" with data from medical imaging can give useful information for understanding human disease, including LC (Figure 9).

ML and deep learning algorithms have been effectively employed in many research contexts to combine diverse omics, imaging, and clinical data [203,204]. Using deep learning models to combine imaging and omics data might aid in early LC diagnosis. Using "radiogenomics," researchers have discovered that high-dimensional features gained from CT scans are connected to the existence of particular mutations in tumor tissues [205]. For example, specific CT scan imaging characteristics, such as anaplastic lymphoma kinase (ALK), EGFR, c-ros oncogene 1 (ROS1), KRAS, and rearranged during transfection proto-oncogene (rearranged during transfection), have been linked to the presence of tumor driving mutations in LC [205–208]. As a result, the extraction, integration, and interpretation of the large volume of data generated by AI-based technologies will be supplemented in a cancer screening program to help its early diagnosis.

4.6 Wearable devices

Wearable materials and devices are one of the specialized areas of therapy and diagnostics that are progressing.

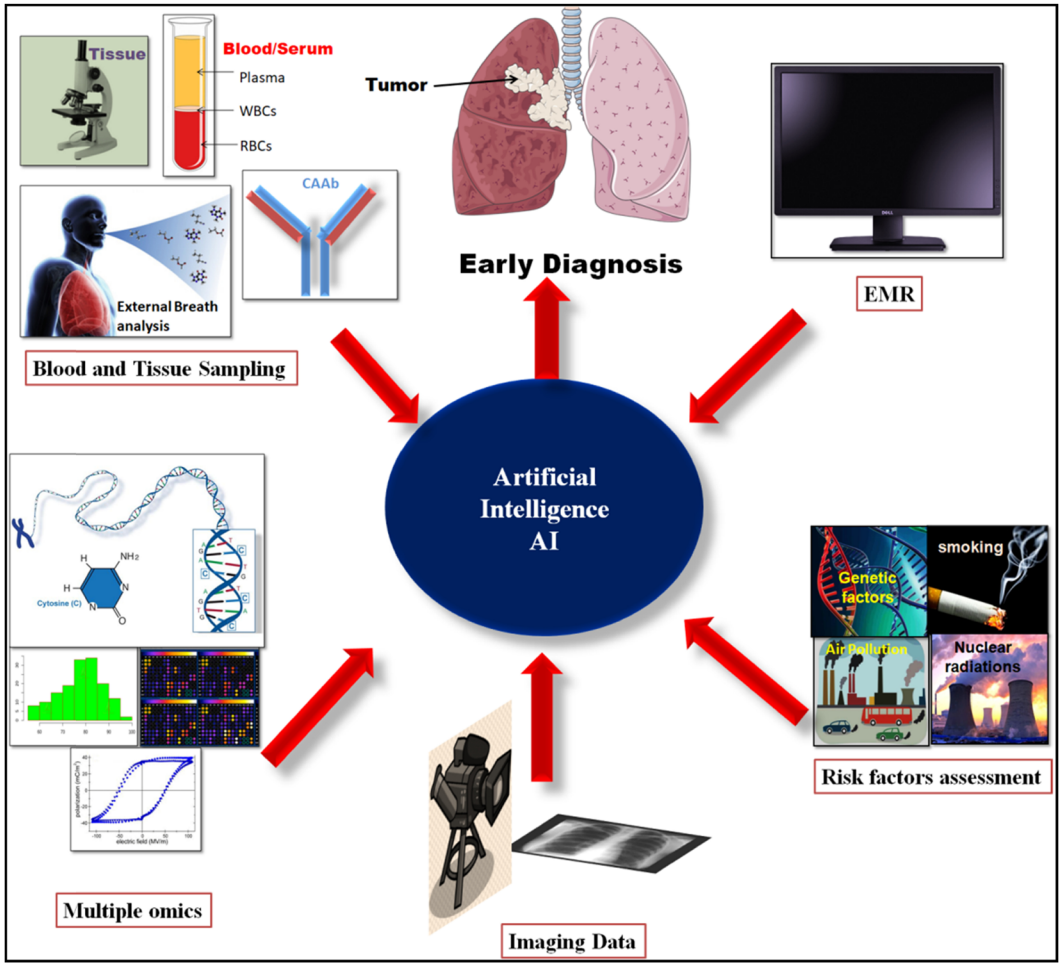

Figure 9: AI algorithms have the ability to enhance the early detection of LC by combining numerous data sources [13].

In terms of point-of-care diagnostics, smartphone-linked applications and sensors, the advent of mobile health have the potential to alter the current healthcare landscape. With more than 95% of the population having access to mobile networks [207], telehealth and mobile health are gaining popularity among academics, and the WHO has formally defined them. A unique self-renewing sensor for detecting VOCs through breath and skin was created in a recent study. This new gold nanoparticle-based sensor has the ability to self-heal injured tissue caused by abrasion [209]. Despite the enormous hurdles that this sector of wearable sensors in oncology faces in terms of development, a large range of smartphone-based applications is accessible [210]. In addition, Cancer Research UK, in partnership with the British Thoracic Society, released "The Pulmonary Nodule Risk App," a smartphone-based tool developed for clinical oncologists to be used for LC evaluation and monitoring [211]. In the realm of LC diagnosis, this area of wearable equipment is underutilized.

The integration of the IoT with cloud computing, big data analytics, and their potentialities in healthcare has resulted in the development of smart health monitoring systems, which have the potential to advance almost every domain of science and technology, and their fusion with nanotechnology is considered the next evolutionary step of the 21st century [15]. For early detection of LC, several real-time-based nano-enabled sensors employ biomarkers found in breath, blood, saliva, and perspiration.

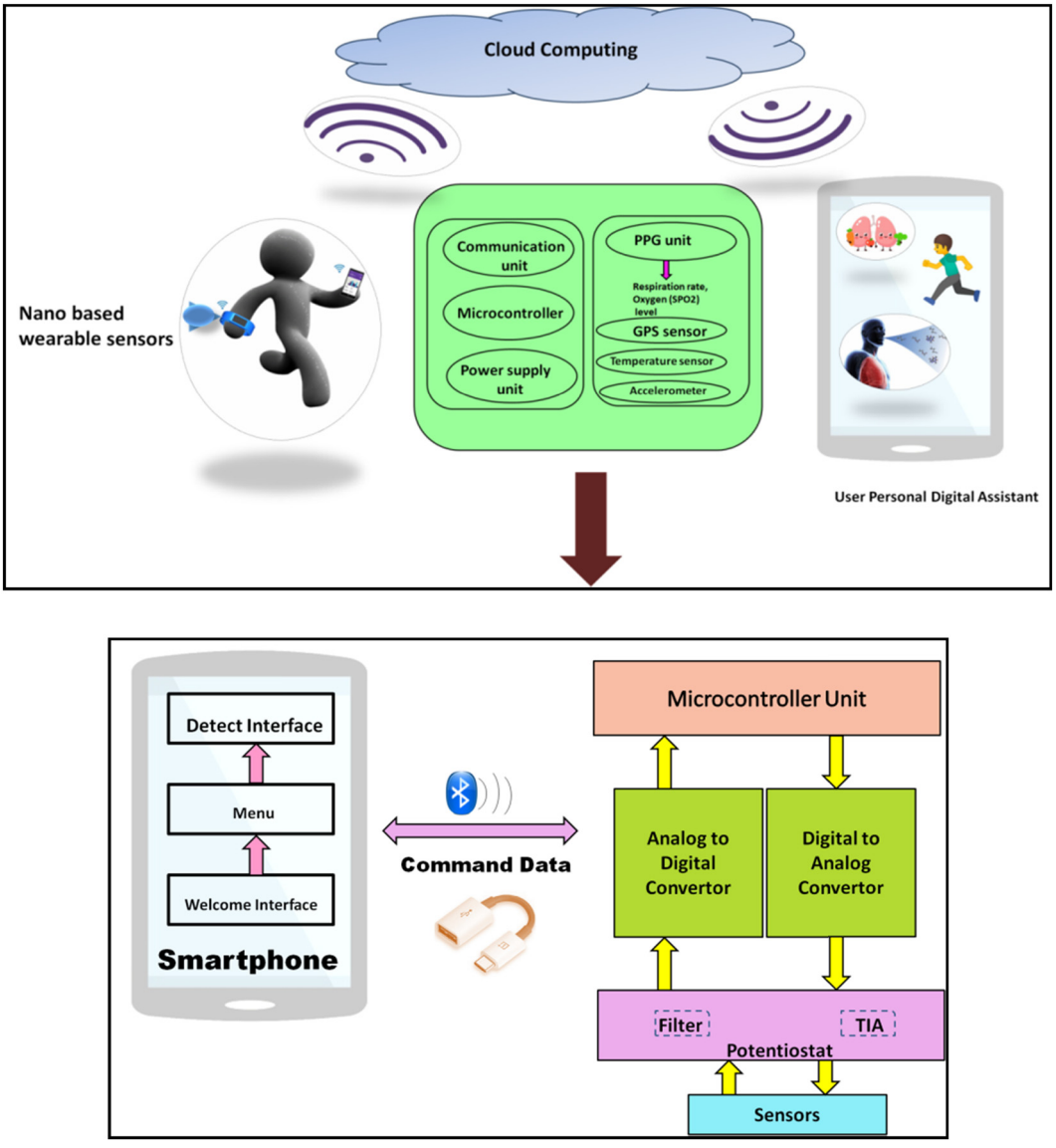

Figure 10: The operational process of the smartphone-associated voltammetry system. Modification of screen-printed electrodes to employ it as the sensor for detection of various samples [15,212]. (Redrawn with permission from Ji *et al.*[212].).

Cloud connectivity is used in these smart healthcare monitoring systems because it provides processing, storage, and data analysis, which aids in informing medical authorities at the right moment. Google has announced the Cloud Healthcare Application Programming Interface, with the goal of making the process of collecting, storing, and accessing healthcare-related data easier for health organizations [15]. Google recently inked a big cloud computing contract with Flex, a publicly traded electronics company that makes medical device components all around the world. Various sensors have been embedded in watches, tattoos, wristbands, cellphones, belts, and soft lenses to gather, monitor, and transmit bodily motions, SPO2 levels, glucose levels, pulse rate, and blood pressure to authorized individuals such as physicians, health businesses, and consultants. Furthermore, by integrating differential pulse voltammetry and cyclic voltammetry, a smartphone-based integrated voltammetry system was created to detect uric acid, ascorbic acid, and dopamine in the body, as shown in Figure 10 [212]. rGO and gold nanoparticles were used to modify the electrodes. The detector turned the analog impulses into digital signals and sent them over Bluetooth to the smartphone. The findings demonstrated that the smartphone-based system could efficiently detect several biomolecules at the same time and that it has promise in point-of-care testing.

5 Conclusion

- In this strategic review, we discussed the conventional methods for LC diagnosis, the recent advancement of MNP-based detection and monitoring systems for prospective LC diagnosis tools, different types of potential MNPs, their synthesis, and the pros and cons for biomedical applications.
- The desirable salient features of MNP-based detection systems along with advanced MNP-based diagnostic tools like biomarkers, microfluidic chips, AI, wearable devices, *etc*., have been summarized.
- Nanoparticles conjugated with targeted agents, biomolecules, antibodies, and other immunomodulatory ligands to increase tumor targeting and develop sustainable systems with low cytotoxicity have been discussed.
- Improvements in the diagnostic systems based on MNPs that will provide early, fast, and better diagnosis of LC cancer have been summarized in detail.
- Moreover, a large number of biomarkers that are in the research pipeline that will add to the specificity of detection systems has been discussed, which will emerge in the field of MNP-based LC detection.
- Further, we discussed how integrating sampling techniques with more advanced technology like 3D-printing and AI will provide fast, efficient, and early-stage diagnosis of LC.
- Integration of conventional and advanced diagnostic tools will overcome the challenges involved in the early detection of LC.

6 Future prospective

In the future, the contribution of the combined effect of clinical trials and biomedicine, materials science, and nanotechnology will certainly overcome the existing challenges in the early diagnosis of LC. Another set of impediments for MNP clinical translation is regulatory and industrial constraints. To overcome these obstacles, a multidisciplinary scheme must be established in conjunction with regulatory authorities to ensure the evaluation and efficacy of nanotechnology. In addition to recent developments in enhancing regulated and sustained drug release, active targeting, and synergistic multimodal methods, MRI monitoring utilizing MNPs has emerged as a possible feature of MNP-based systems. An increase in appropriate preclinical research is predicted to be required to accelerate the development of magnetic nanoplatforms for early, rapid, and efficacious diagnostics. The trend of research institutes building multidisciplinary nanotechnology centers and regulatory bodies adopting standards relevant to nanoparticle platforms will make this achievable. The interconnections and networking of smart objects with IoT solutions, which cover various communication technologies such as Bluetooth, Wi-Fi, Zigbee, radio frequency identification, and others, to build realistic and functioning IoT applications, is the main challenge faced during the development of low-cost technology-enabled care.

Funding information: Rajiv Manohar is thankful to UGC for "MID CAREER AWARD" [No. F.19-224/2018 (BSR)] and Centre of Excellence at APJ Abdul Kalam Centre for Innovation, University of Lucknow. Avanish Singh Parmar is thankful to the Department of Science and Technology (SERB), India – CRG/2019/000903 (Core Research Grant) & SB/S2/RJN-140/2014 (Ramanujan Fellowship Award) for the financial assistance.

Author contributions: Ayushi Rastogi: writing – original draft, writing – review and editing. Kanchan Yadav: writing, review, and formatting. Archana Mishra: conceptualization, resources, writing – original draft, writing – review and

editing. Manu Smriti Singh: writing – review and editing. Shilpi Chaudhary: writing – review and editing. Rajiv Manohar: conceptualization, validation, methodology, resources, writing – review and editing. Avanish Singh Parmar: conceptualization, visualization, validation, methodology, resources, writing – review and editing. All authors have accepted responsibility for the entire content of this manuscript and approved its submission.

Conflict of interest: The authors state no conflict of interest.

References

[1] Sung H, Ferlay J, Siegel RL, Laversanne M, Soerjomataram I, Jemal A, et al. Global cancer statistics 2020: globocan estimates of incidence and mortality worldwide for 36 cancers in 185 countries. CA Cancer J Clin. 2021;71(3):209–49.

[2] WHO report on cancer; 2020.

[3] Lin L, Yan L, Liu Y, Yuan F, Li H. Incidence and death in 29 cancer groups in 2017 and trend analysis from 1990 to 2017 from the global burden of disease study. J Hematol Oncol. 2019;9:1–21.

[4] Bray F, Ferlay J, Soerjomataram I. Global cancer statistics 2018: globocan estimates of incidence and mortality worldwide for 36 cancers in 185 countries. CA Cancer J Clinc. 2018;68(6):394–424.

[5] Lemjabbar-Alaoui H, Hassan OUI, Yang YW, Buchanan PP. Lung cancer: biology and treatment options. BiochimBiophys Acta. 2015;1856(2):189–210.

[6] Dürr S, Janko C, Lyer S, Tripal P, Schwarz M, Zaloga J, et al. Magnetic nanoparticles for cancer therapy. Nanotech Rev. 2013;2:395–409.

[7] Gkountas AA, Polychronopoulos ND, Sofiadis GN, Karvelas EG, Spyrou LA, Sarris IE. Simulation of magnetic nanoparticles crossing through a simplified blood-brain barrier model for glioblastoma multiforme treatment. Computer methods Prog Biomed. 2021;212:106477.

[8] Hosu O, Tertis M, Cristea C. Implication of magnetic nanoparticles in cancer detection, screening and treatment. Magnetochemistry. 2019;5(4):55.

[9] Guo QR, Zhang LL, Liu JF, Li Z, Li JJ, Zhou WM, et al. Multifunctional microfluidic chip for cancer diagnosis and treatment. Nanotheranostics. 2021;5(1):73–89.

[10] Shende P, Augustine S, Prabhakar B, Gaud RS. Advanced multimodal diagnostic approaches for detection of lung cancer. Expert Rev Mol Diagnostics. 2019;19:409–17.

[11] Jin C, Wang K, Oppong-gyebi A, Hu J. Application of nanotechnology in cancer diagnosis and therapy – a mini-review. Int J Med Sci. 2020;17(18):2964–73.

[12] Chouhan RS, Horvat M, Ahmed J, Alhokbany N, Alshehri SM, Gandhi S. Magnetic nanoparticles–a multifunctional potential agent for diagnosis and therapy. Cancers. 2021;13:2213.

[13] Espinoza JL, Dong LT. Artificial intelligence tools for refining lung cancer screening. J Clin Med. 2020;9:3860.

[14] Dlamini Z, Francies FT, Hull R, Marima R. Artificial intelligence (AI) and big data in cancer and precision oncology. Comput Struct Biotechnol J. 2020;18:2300–11.

[15] Singh KR, Nayak V, Singh J, Singh RP. Nano-enabled wearable sensors for the internet of things (IoT). Mater Lett. 2021;304:130614.

[16] Luo Z, Du H. Prospect of different types of magnetic nanoparticles in stem cell therapy. Stem Cell Rev Rep. 2020;16:675–83.

[17] Petrarca C, Poma AM, Vecchiotti G, Bernardini G, Niu Q, Cattaneo AG, et al. Cobalt magnetic nanoparticles as theranostics: conceivable or forgettable? Nanotech Rev. 2020;9:1522–38.

[18] Jaji ND, Lee HL, Hussin MH, Akil HM, Zakaria MR, Othman MBH. Advanced nickel nanoparticles technology: From synthesis to applications. Nanotech Rev. 2020;9:1456–80.

[19] Ahghari MR, Soltaninejad V, Maleki A. Synthesis of nickel nanoparticles by a green and convenient method as a magnetic mirror with antibacterial activities. Sci Rep. 2020;10:12627.

[20] Ali A, Zafar H, Zia M, Haq IU, Phull AR, Ali JS, et al. Synthesis, characterization, applications, and challenges of iron oxide nanoparticles. Nanotech Sci Appl. 2016;9:49–67.

[21] Shi Y, Lin M, Jiang X, Liang S. Recent advances in FePt nanoparticles for biomedicine. J Nanomat. 2015;2015:467873.

[22] Sato K, Konno TJ, Hirotsu Y. Electron microscopy studies on magnetic l_{10} – type FePd nanoparticles. Chapter 4. Adv Imaging Electron Phys. 2012;170:165–225.

[23] Van NTT, Trung TT, Nam NH, Phu ND, Hai NH, Luong NH. Hard magnetic properties of FePd nanoparticles. Eur Phys J Appl Phys. 2013;64:10403.

[24] Barrera G, Scaglione F, Cialone M, Celegato F, Coïsson M, Rizzi P, et al. Structural and magnetic properties of fepd thin film synthesized by electrodeposition method. Mater. 2020;13:1454.

[25] Malinowska I, Ryżyńska Z, Mrotek E, Klimczuk T, Jurek AZ. Synthesis of $CoFe_2O_4$nanoparticles: the effect of ionic strength, concentration, and precursor type on morphology and magnetic properties. J Nanomat. 2020;2020:9046219.

[26] Shabani M, Saebnoori E, Hassanzadeh-tabrizi SA. Bakhsheshi – Rad HR. Novel synthesis of nickel ferrite magnetic nanoparticles by an in-liquid plasma. J Mater Sci: Mater Electron. 2021;32:10424–442.

[27] Alhadlaq HA, Akhtar MJ, Ahamed M. Zinc ferrite nanoparticle-induced cytotoxicity and oxidative stress in different human cells. CellBiosci. 2015;5:55.

[28] Islam K, Haque M, Kumar A, Hoq A, Hyder F, Hoque SM. Manganese ferrite nanoparticles ($MnFe_2O_4$): size dependence for hyperthermia and negative/positive contrast enhancement in MRI. Nanomat. 2020;10:2297.

[29] Kuznetsov MV, Morozov YG, Belousova OV. Synthesis of copper ferrite nanoparticles. Inorg Mater. 2013;49:606–15.

[30] Ye Z, Deng Z, Zhang L, Chen J, Wang G, Wu Z. The structure of copper ferrite prepared by five methods and its catalytic activity on lignin oxidative degradation. Mater Res Express. 2020;7:035007.

[31] Meidanchi A, Ansari H. Copper spinel ferrite superparamagnetic nanoparticles as a novel radiotherapy enhancer effect in cancer treatment. J Clust Sci. 2021;32:657–63.

[32] Suharyadi E, Hermawan A, Puspitarum DL. Crystal structure and magnetic properties of magnesium ferrite ($MgFe_2O_4$) nanoparticles synthesized by coprecipitation method. IOP Conf Ser: J Phys: Conf Series. 2018;1091:012003.
[33] Cristea C, Tertis M, Galatus R. Magnetic nanoparticles for antibiotics detection. Nanomater. 2017;7:119.
[34] Xu JK, Zhang FF, Sun JJ, Sheng J, Wang F, Sun M. Bio and nanomaterials based on Fe_3O_4. Mol. 2014;19(12):21506–28.
[35] Chen Z, Wu C, Zhang Z, Wu W, Wang X, Yu Z. Synthesis, functionalization, and nanomedical applications of functional magnetic nanoparticles. Chin Chem Lett. 2018;29(11):1601–08.
[36] Liu C, Zou B, Rondinone AJ, Zhang ZJ. Reverse micelle synthesis and characterization of superparamagnetic $MnFe_2O_4$ spinel ferrite nanocrystallites. J Phys Chem B. 2000;104:1143–5.
[37] Karade VC, Dongale TD, Sahoo SC, Subasa C, Kollu P, Chougale AD, et al. Effect of reaction time on structural and magnetic properties of green-synthesized magnetic nanoparticles. J Phys Chem Solids. 2018;120:161–6.
[38] Magdziarz A, Colmenares JC. In situ coupling of ultrasound to electro-and photo-deposition methods for materials synthesis. Mol. 2017;22:216.
[39] Abd Elrahman AA, Mansour FR. Targeted magnetic iron oxide nanoparticles: preparation, functionalization and biomedical application. J Drug Deliv Sci Technol. 2019;52:702–12.
[40] Katz E. Synthesis, properties and applications of magnetic nanoparticles and nanowires – a brief introduction. Magnetochemistry. 2019;5(4):61.
[41] Cores J, Caranasos T, Cheng K. Magnetically targeted stem cell delivery for regenerative medicine. J Funct Biomater. 2015;6:526–46.
[42] Lu CW, Hung Y, Hsiao JK, Yao M, Chung TH, Lin YS, et al. Bifunctional magnetic silica nanoparticles for highly efficient human stem cell labeling. Nano Lett. 2007;7:149–54.
[43] Tang F, Li L, Chen D. Mesoporous silica nanoparticles: Synthesis, biocompatibility and drug delivery. Adv Mater. 2012;24:1504–34.
[44] Marty J. Nanoparticles-a new colloidal drug delivery system. Pharma Acta Helv. 1978;53:17–23.
[45] Xie L, Tong W, Yu D, Xu J, Li J, Gao C. Bovine serum albumin nanoparticles modified with multilayers and aptamers for pH-responsive and targeted anti-cancer drug delivery. J Mater Chem. 2012;22:6053–60.
[46] Stamopoulos D, Gogola V, Manios E, Gourn E, Benaki D, Niarchos D, et al. Biocompatibility and solubility of Fe_3O_4-BSA conjugates with human blood. Curr Nanosci. 2009;5:177–81.
[47] Kim TH, Kim JK, Shim W, Kim SY, Park TJ, Jung J. Tracking of transplanted mesenchymal stem cells labeled with fluorescent magnetic nanoparticle in liver cirrhosis rat model with 3-T MRI. Magnetic Reson Imaging. 2010;28:1004–13.
[48] Frank JA, Miller BR, Arbab AS, Zywicke HA, Jordan EK, Lewis BK, et al. Clinically applicable labeling of mammalian and stem cells by combining superparamagnetic iron oxides and transfection agents. Radiol. 2003;228:480–87.
[49] Arbab AS, Bashaw LA, Miller BR, Jordan EK, Lewis BK, Kalish H, et al. Characterization of biophysical and metabolic properties of cells labeled with superparamagnetic iron oxide nanoparticles and transfection agent for cellular MR imaging. Radiol. 2003;229:838–46.
[50] Illés E, Tombácz E, Szekeres M, Tóth IY, Szabó Á, Iván B. Novel carboxylated PEG-coating on magnetite nanoparticles designed for biomedical applications. J Magnetism Magnetic Mater. 2015;380:132–9.
[51] Landázuri NS, Tong JS, Joseph G, Weiss D, Sutcliffe DJ, Giddens DP, et al. Magnetic targeting of human mesenchymal stem cells with internalized superparamagnetic iron oxide nanoparticles. Small. 2013;9:4017–26.
[52] Cheng K, Shen D, Hensley MT, Middleton R, Sun B, Liu W, et al. Magnetic antibody-linked nanomatchmakers for therapeutic cell targeting. Nat Comm. 2014;5:4880.
[53] Hernández AD, Gracida J, García-Almendárez BE, Regalado C, Núñez R, Amaro-Reyes A. Characterization of magnetic nanoparticles coated with chitosan: a potential approach for enzyme immobilization. J Nanomater. 2018;11:9468574.
[54] Lin KYA, Hsu FK, Lee WD. Magnetic cobalt–graphene nanocomposite derived from self-assembly of MOFs with graphene oxide as an activator for peroxymonosulfate. J Mater Chem A. 2015;3:9480.
[55] Hatamie S, Ahadian MM, Ghiass MA, zad AI, Reza S, Benyamin P, et al. Graphene/cobalt nanocarrier for hyperthermia therapy and MRI diagnosis. Colloids Surf B. 2016;146:271–9.
[56] Linemann T, Thomsen LB, du Jardin KG, Laursen JC, Jensen JB, Lichota J, et al. Development of a novel lipophilic, magnetic nanoparticle for *in vivo* drug delivery. Pharmaceutics. 2013;5:246–60.
[57] Kernstine KH, Stanford W, Mullan BF, Rossi NP, Thompson BH, Bushnell DL, et al. PET, CT, and MRI with combidex for mediastinal staging in non-small cell lung carcinoma. Ann Thorac Surg. 1999;68:1022–8.
[58] Harisinghani MG, Saini S, Weissleder R, Hahn PF, Yantiss RK, Tempany C, et al. MR lymphangiography using ultrasmall superparamagnetic iron oxide in patients with primary abdominal and pelvic malignancies: Radiographicpathologiccorrelation. Americ J Roentgenol. 1999;172:1347–51.
[59] Reimer P, Balzer T. Ferucarbotran (Resovist): a new clinically approved RES-specific contrast agent for contrast-enhanced MRI of the liver: properties, clinical development, and applications. Eur Radiol. 2003;13:1266–76.
[60] Vogl TJ, Hammerstingl R, Schwarz W, Kümmel S, Müller PK, Balzer T, et al. Magnetic resonance imaging of focal liver lesions: Comparison of the superparamagnetic iron oxide resovist versus gadolinium-DTPA in the same patient. Invest Radiol. 1996;31(11):696–708.
[61] Reimer P, Rummeny EJ, Daldrup HE, Balzer T, Tombach B, Berns T, et al. Clinical results with Resovist: a phase 2 clinical trial. Radiol. 1995;195(2):489–96.
[62] Kostura L, Kraitchman DL, Mackay AM, Pittenger MF, Bulte JMW. Feridex labeling of mesenchymal stem cells inhibits chondrogenesis but not adipogenesis or osteogenesis. NMR Biomed. 2004;17(7):513–7.
[63] Briley-Saebo KC, Mani V, Hyafil F, Cornily JC, Fayad ZA. Fractionated Feridex and positive contrast: *In vivo* MR imaging of atherosclerosis. Magn Reson Med. 2008;59(4):721–30.

[64] Johnson L, Pinder SE, Douek M. Deposition of superparamagnetic iron-oxide nanoparticles in axillary sentinel lymph nodes following subcutaneous injection. Histopathology. 2013;62(3):481–6.
[65] Bullivant JP, Zhao S, Willenberg BJ, Kozissnik B, Batich CD, Dobson J. Materials characterization of feraheme/ferumoxytol and preliminary evaluation of its potential for magnetic fluid hyperthermia. Int J Mol Sci. 2013;14(9):17501–10.
[66] Kellar KE, Fujii DK, Gunther WHH, Briley-Sæbø K, Spiller M, Koenig SH. 'NC100150', a preparation of iron oxide nanoparticles ideal for positive-contrast MR angiography. J Mag Res Imag. 2000;11:488–94.
[67] Shan L, Leung K, Zhang H, Cheng K. MP-B, 2004 undefined. Molecular imaging and contrast agent database (micad). bethesda (md) national center for biotechnology information (us) 2004–2013. Available online: europepmc.org
[68] Polychronopoulos ND, Gkountas AA, Sarris IE, Spyrou LA. A computational study on magnetic nanoparticles hyperthermia of ellipsoidal tumors. Appl Sci. 2021;11:9526.
[69] Knight SB, Crosbie PA, Balata H, Chudziak J, Hussell T, Dive C. Progress and prospects of early detection in lung cancer. Open Biol. 2017;7:170070.
[70] Tang X, Wang Z, Wei F, Mu W, Han X. Recent progress of lung cancer diagnosis using nanomaterials. Cryst. 2021;11:24.
[71] Jalal AH, Sikder AK, Alam F, Samin S, Rahman SS, Khan MMA, et al. Early diagnosis with alternative approaches: innovation in lung cancer care. Shanghai Chest. 2021;5(7):1–14.
[72] Senyei A, Widder K, Czerlinski C. Magnetic guidance of drug carrying microspheres. J Appl Phys. 1978;49:3578–83.
[73] Dames P, Gleich B, Flemmer A, Hajek K, Seidl N, Wiekhorst F, et al. Targeted delivery of magnetic aerosol droplets to the lung. Nat Nanotech. 2007;2:495–9.
[74] Plank C. Nanomagnetosols: magnetism opens up new perspectives for targeted aerosol delivery to the lung. Trends Biotech. 2021;26:2.
[75] Abdeen S, Praseetha PK. Diagnostics and treatment of metastatic cancers with magnetic nanoparticles. J Nanomed Biother Discov. 2013;3:115.
[76] Fallahzadeh S, Bahrami H, Akbarzadeh A, Tayarani M. High-isolation dual-frequency operation patch antenna using spiral defected microstrip structure. IEEE Antennas Wirel Propag Lett. 2010;9:122–4.
[77] Anderson JM, Shive MS. Biodegradation and biocompatibility of PLA and PLGA microspheres. Adv Drug Deliv Rev. 2012;64:72–82.
[78] Mahmoudi M, Laurent S, Shokrgozar MA, Hosseinkhani M. Toxicity evaluations of superparamagnetic iron oxide nanoparticles: cell 'vision' versus physicochemical properties of nanoparticles. ACS Nano. 2011;5(9):7263–76.
[79] Soppimath KS, Aminabhavi TM, Kulkarni AR, Rudzinski WE. Biodegradable polymeric nanoparticles as drug delivery devices. J Control Rel. 2001;70:1–20.
[80] Ziarani GM, Malmir M, Lashgari N, Badiei A. The role of hollow magnetic nanoparticles in drug delivery. RSC Adv. 2019;9:25094–106.
[81] Mukherjee S, Liang L, Veiseh O. Recent advancements of magnetic nanomaterials in cancer therapy. Pharmaceutics. 2020;12:147.
[82] Yang BY, Moon SH, Seelam SR, Jeon MJ, Lee YS, Lee DS, et al. Development of a multimodal imaging probe by encapsulating iron oxide nanoparticles with functionalized amphiphiles for lymph node imaging. Nanomed. 2015;10:1899–910.
[83] Xu J, Li P, Fan Y. Preparation of magnetic-fluorescent bifunctional microrods as a drug delivery system via one-step electrospraying. Proceedings. 2021;78:44.
[84] Guan Y, Yang Y, Wang X, Yuan H, Yang Y, Li N, et al. Multifunctional Fe_3O_4 @ SiO_2 -CDs magnetic fluorescent nanoparticles as effective carrier of gambogic acid for inhibiting VX2 tumor cells. J Mol Liq. 2021;327:114783.
[85] Heuer-jungemann A, Feliu N, Bakaimi I, Hamaly M, Alkilany A, Chakraborty I, et al. The role of ligands in the chemical synthesis and applications of inorganic nanoparticles. Chem Rev. 2019;119:4819–80.
[86] Zhao J, Wallace M, Melancon MP. Cancer theranostics with gold nanoshells. Nanomed. 2014;9(13):2041–57.
[87] Nunes T, Pons T, Hou X, Do KV, Caron B, Rigal M, et al. Pulsed-laser irradiation of multifunctional gold nanoshells to overcome trastuzumab resistance in HER2-overexpressing breast cancer. J Exp Clin Cancer Res. 2019;38(1):1–13.
[88] Fu N, Hu Y, Shi S, Ren S, Liu W, Su S, et al. Wang, Au nanoparticles on two-dimensional MoS2 nanosheets as a photoanode for efficient photoelectrochemical miRNA detection. Analyst. 2018;143(7):1705–12.
[89] Qian J, Yang X, Jiang L, Zhu C, Mao H, Wang K. Facile preparation of Fe3O4 nanospheres/reduced graphene oxide nanocomposites with high peroxidase-like activity for sensitive and selective colorimetric detection of acetylcholine. Sens Actuators, B Chem. 2014;201:160–6.
[90] Gao L, Wu J, Lyle S, Zehr K, Cao L, Gao D. Magnetite nanoparticle-linked immunosorbent assay. J Phys Chem C. 2008;112(44):17357–61.
[91] Islam S, Colt HG, Finlay G. Flexible bronchoscopy in adults: Preparation, procedural technique, and complications. Netherlands: Wolters Kluwer Health; 2016.
[92] Kamath AV, Chhajed PN. Role of bronchoscopy in early diagnosis of lung cancer. Indian J Chest Dis Allied Sci. 2006;48:265.
[93] Herth FJ. Bronchoscopic techniques in diagnosis and staging of lung cancer. Breathe. 2011;7:324–7.
[94] Spiro SG, Hackshaw A. Research in progress–LungSEARCH: a randomised controlled trial of surveillance for the early detection of lung cancer in a high-risk group. Thorax. 2016;71:91–3.
[95] UC San Diego Health. Endobronchial Ultrasound Bronchoscopy (EBUS). Published in 2018. Available online: https://health.ucsd.edu/specialties/pulmonary/procedures/Pages/endobronchial.aspx.
[96] Comino RMO, Gil D, Minchole E, Ferrer MD, Cubero N, Lisbona RL, et al. MA 20.08 Classification of confocal endomicroscopy patterns for diagnosis of lung cancer. J Thorac Oncol. 2017;12:S1889.
[97] Cormode DP, Naha PC, Fayad ZA. Nanoparticle contrast agents for computed tomography: a focus on micelles. Contrast Media Mol Imag. 2014;9:37–52.
[98] Thomas R, Park IK, Jeong YY. Magnetic iron oxide nanoparticles for multimodal imaging and therapy of cancer. Int J Mol Sci. 2013;14:15910–30.
[99] Naha PC, Al Zaki A, Hecht E, Chorny M, Chhour P, Blankemeyer E, et al. Dextran coated bismuth-iron oxide nanohybrid contrast agents for computed tomography and magnetic resonance imaging. J Mat Chem B. 2014;46:8239–48.

[100] Xue S, Wang Y, Wang M, Zhang L, Du X, Gu H, et al. Iodinated oil-loaded, fluorescent mesoporous silica-coated iron oxide nanoparticles for magnetic resonance imaging/computed tomography/fluorescence trimodal imaging. Int J Nanomed. 2014;9:2527–34.
[101] Reguera J, Jiménez D, Aberasturi D, Henriksen-Lacey M, Langer J, Espinosa A, et al. Janus plasmonic-magnetic gold-iron oxide nanoparticles as contrast agents for multimodal imaging. Nanoscale. 2017;9:9467–80.
[102] Weissleder R, Nahrendorf M, Pittet MJ. Imaging macrophages with nanoparticles. Nat Mater. 2014;13:125–38.
[103] Thorsson V, Gibbs DL, Brown SD, Wolf D, Bortone DS, Yang TH, et al. The immune landscape of cancer. Immunity. 2018;48:812–30.e14.
[104] Sanhai WR, Sakamoto JH, Canady R, Ferrari M. Seven challenges for nanomedicine. Nat Nanotechnol. 2008;3:242–4.
[105] Kim HY, Li R, Ng TSC, Courties G, Rodell CB, Prytyskach M, et al. Quantitative imaging of tumor-associated macrophages and their response to therapy using Cu-64-labeled macrin. ACS Nano. 2018;12:12015–29.
[106] Li L, Jiang W, Luo K, Song H, Lan F, Wu Y, et al. Superparamagnetic iron oxide nanoparticles as MRI contrast agents for non-invasive stem cell labeling and tracking. Theranostics. 2013;3:595–615.
[107] Wang G, Gao W, Zhang X, Mei X. Au nanocage functionalized with ultra-small Fe_3O_4 nanoparticles for targeting t1-t2 dual MRI and CT imaging of tumor. Sci Rep. 2016;28258.
[108] Sim AJ, Kaza E, Singer L, Rosenberg SA. A review of the role of MRI in diagnosis and treatment of early-stage lung cancer. Clin Transl Radiat Oncol. 2020;24:16–22.
[109] Wild JM, Marshall H, Bock M, Schad LR, Jakob PM, Puderbach M, et al. MRI of the lung (1/3): methods. Insights Imaging. 2012;3:345–53.
[110] Bianchi A, Dufort S, Lux F, Fortin PY, Tassali N, Tillement O, et al. Targeting and *in vivo* imaging of non-small-cell lung cancer using nebulized multimodal contrast agents. Proc Natl Acad Sci USA. 2014;111:9247–52.
[111] Huang X, Yuan Y, Ruan W, Liu L, Liu M, Chen S, et al. pH-responsive theranostic nanocomposites as synergistically enhancing positive and negative magnetic resonance imaging contrast agents. J Nanobiotech. 2018;16(1):30.
[112] Xia L, Guo X, Liu T, Xu X, Jiang J, Wang F, et al. Multimodality imaging of naturally active melanin nanoparticles targeting somatostatin receptor subtype 2 in human small-cell lung cancer. Nanoscale. 2019;11(30):14400–9.
[113] Weizenecker J, Gleich B, Rahmer J, Dahnke H, Borgert J. Three-dimensional real-time in vivo magnetic particle imaging. Phys Med Biol. 2009;54(5):L1–10.
[114] Tomitaka A, Arami H, Gandhi S, Krishnan KM. Lactoferrin conjugated iron oxide nanoparticles for targeting brain glioma cells in magnetic particle imaging. Nanoscale. 2015;7:16890–8.
[115] Gandhi S, Arami H, Krishnan KM. Detection of cancer-specific proteases using magnetic relaxation of peptide-conjugated nanoparticles in biological environment. Nano Lett. 2016;16:3668–74.
[116] Travis WD, Brambilla E, Nicholson AG, Yatabe Y, Austin JHM, Beasley MB. WHO Panel, The 2015 world health organization classification of lung tumors. J Thorac Oncol. 2015;10:1243.
[117] Zamay TN, Zamay GS, Kolovskaya OS, Zukov RA, Petrova MM, Gargaun A, et al. Current and prospective protein biomarkers of lung cancer. Cancers (Basel). 2017;9:1–22.
[118] Li P, Shi JX, Xing MT, Dai LP, Li JT, Zhang JY. Evaluation of serum autoantibodies against tumor-associated antigens as biomarkers in lung cancer. Tumor Biol. 2017;39:1010428317711662.
[119] Ajona D, Castaño Z, Garayoa M, Zudaire E, Pajares MJ, Martinez A, et al. Expression of complement factor H by lung cancer cells: Effects on the activation of the alternative pathway of complement. Cancer Res. 2004;64:6310.
[120] Ajona D, Pajares MJ, Corrales L, Perez-Gracia JL, Agorreta J, Lozano MD, et al. Investigation of complement activation product C4d as a diagnostic and prognostic biomarker for lung cancer. J Natl Cancer Inst. 2013;105:1385.
[121] Elazezy M, Joosse SA. Techniques of using circulating tumor DNA as a liquid biopsy component in cancer management. Comput Struct Biotechnol J. 2018;16:370–8.
[122] Doseeva V, Colpitts T, Gao G, Woodcock J, Knezevic V. Performance of a multiplexed dual analyte immunoassay for the early detection of non-small cell lung cancer. J Transl Med. 2015;13:55.
[123] Luo W, Rao M, Qu J, Luo D. Applications of liquid biopsy in lung cancer-diagnosis, prognosis prediction, and disease monitoring. Am J Transl Res. 2018;10:3911–23.
[124] Hofman P. Liquid biopsy for early detection of lung cancer. Curr Opin Oncol. 2017;29:73–8.
[125] Santarpia M, Liguori A, D'Aveni A, Karachaliou N, Cao MG, Daffinà MG, et al. Liquid biopsy for lung cancer early detection. J Thorac Dis. 2018;10:S882–97.
[126] Xie Y, Todd NW, Liu Z, Zhan M, Fang H, Peng H, et al. Altered mirna expression in sputum for diagnosis of non-small cell lung cancer. Lung Cancer. 2010;67:170–6.
[127] Skog J, Wurdinger T, Rijn SV, Meijer D, Gainche L, Esteves MS, et al. Glioblastoma microvesicles transport RNA and proteins that promote tumor growth and provide diagnostic biomarkers. Nat Cell Biol. 2008;10:1470–6.
[128] Salido-Guadarrama I, Romero-Cordoba S, Peralta-Zaragoza O, Hidalgo-Miranda A, Rodriguez-Dorantes M. MicroRNAs transported by exosomes in body fluids as mediators of intercellular communication in cancer. Onco Targets Ther. 2014;7:1327–38.
[129] Wozniak MB, Scelo G, Muller DC, Mukeria A, Zaridze D, Brennan P. Circulating MicroRNAs as noninvasive biomarkers for early detection of nonsmall-cell lung cancer. PLoS One. 2015;10:e0125026.
[130] Powrozek T, Krawczyk P, Kowalski DM, Winiarczyk K, Olszyna-Serementa M, Milanowski J. Plasma circulating microRNA-944 and microRNA-3662 as potential histologic type-specific early lung cancer biomarkers. Transl Res. 2015;166:315–23.
[131] Shen J, Todd NW, Zhang H, Yu L, Lingxiao X, Mei Y, et al. Plasma microRNAs as potential biomarkers for non-small-cell lung cancer. Lab Invest. 2011;91:579–87.
[132] Shen J, Liu Z, Todd NW, Zhang H, Liao J, Yu L, et al. Diagnosis of lung cancer in individuals with solitary pulmonary nodules by plasma microRNA biomarkers. BMC Cancer. 2011;11:374.
[133] Boeri M, Verri C, Conte D, Roz L, Modena P, Facchinetti F, et al. MicroRNA signatures in tissues and plasma predict development and prognosis of computed tomography

detected lung cancer. Proc Natl Acad Sci USA. 2011;108:3713–8.
[134] Bach PB, Jett JR, Pastorino U, Tockman MS, Swensen SJ, Begg CB. Computed tomography screening and lung cancer outcomes. JAMA. 2007;297:953–61.
[135] Pastorino U, Rossi M, Rosato V, Marchianò A, Sverzellati N, Morosi C, et al. Annual or biennial CT screening versus observation in heavy smokers: 5-year results of the MILD trial. Eur J Cancer Prev. 2012;21:308–15.
[136] Sozzi G, Boeri M, Rossi M, Verri C, Suatoni P, Bravi F, et al. Clinical utility of a plasma-based miRNA signature classifier within computed tomography lung cancer screening: a correlative MILD trial study. J Clin Oncol. 2014;32:768–73.
[137] Xing L, Su J, Guarnera MA, Zhang H, Cai L, Zhou R, et al. Sputum microRNA biomarkers for identifying lung cancer in indeterminate solitary pulmonary nodules. Clin Cancer Res. 2015;21:484–9.
[138] Su Y, Fang HB, Jiang F. Integrating DNA methylation and microRNA biomarkers in sputum for lung cancer detection. Clin Epigenetics. 2016;8:1–9.
[139] Su J, Liao J, Gao L, Shen J, Guarnera MA, Zhan M, et al. Analysis of small nucleolar RNAs in sputum for lung cancer diagnosis. Oncotarget. 2015;7:5131–42, Available from http://www.impactjournals.com/oncotarget/index.php?journal=oncotarget&page=article&op=view&path%5B%5D=4219&path%5B%5D=9352.
[140] Heitzer E, Ulz P, Geigl JB. Circulating tumor DNA as a liquid biopsy for cancer. Clin Chem. 2015;61:112–23.
[141] Newman AM, Bratman SV, To J, Wynee JF, Eclov NCW, Modlin LA, et al. An ultrasensitive method for quantitating circulating tumor DNA with broad patient coverage. Nat Med. 2014;20:548–54.
[142] Gormally E, Vineis P, Matullo G, Veglia F, Caboux E, Roux EL. TP53 and KRAS2 mutations in plasma DNA of healthy subjects and subsequent cancer occurrence: a prospective study. Cancer Res. 2006;66:6871–6.
[143] Cuesta LF, Perdomo S, Avogbe PH, Leblay N, Delhomme TM, Gaborieau V. Identification of circulating tumor DNA for the early detection of small-cell lung cancer. EBioMedicine. 2016;10:117–23.
[144] Sozzi G, Conte D, Leon ME, Ciricione R, Roz L, Ratcliffe C, et al. Quantification of free circulating DNA as a diagnostic marker in lung cancer. J Clin Oncol. 2003;21:3902–8.
[145] Sozzi G, Roz L, Conte D, Mariani L, Andriani F, Vullo SL, et al. Plasma DNA quantification in lung cancer computed tomography screening: five year results of a prospective study. Am J Respir Crit Care Med. 2009;179:69–74.
[146] Ulivi P, Casoni GL, Foschi G, Scarpi E, Tomassetti S, Romagnoli M, et al. MMP-7 and fcDNA serum levels in early NSCLC and idiopathic interstitial pneumonia: preliminary study. Int J Mol Sci. 2013;14(24):24097–112.
[147] Abbosh C, Birkbak NJ, Wilson GA, Hanjani MJ, Constantin T, Salari R, et al. TRACERx consortium; PEACE consortium; Charles Swanton, Phylogenetic ctDNA analysis depicts early-stage lung cancer evolution. Nature. 2017;545:446–51.
[148] Hagiwara N, Mechanic LE, Trivers GE, Cawley HL, Taga M, Bowman ED, et al. Quantitative detection of p53 mutations in plasma DNA from tobacco smokers. Cancer Res. 2006;66:8309–17.
[149] Yadav VK, DeGregori J, De S. The landscape of somatic mutations in protein coding genes in apparently benign human tissues carries signatures of relaxed purifying selection. Nucleic Acids Res. 2016;44:2075–84.
[150] Kolbl AC, Jeschke U, Andergassen U. The significance of epithelial-to-mesenchymal transition for circulating tumor cells. Int J Mol Sci. 2016;17:1308.
[151] Labelle M, Hynes RO. The initial hours of metastasis: the importance of cooperative host–tumor cell interactions during hematogenous dissemination. Cancer Discov. 2012;2:1091–9.
[152] Williamson SC, Williamson SC, Metcalf RL, Trapani F, Mohan S, Antonello J, et al. Vasculogenic mimicry in small cell lung cancer. Nat Commun. 2016;7:13322.
[153] Yang MH, Imrali A, Heeschen C. Circulating cancer stem cells: the importance to select. Chin J Cancer Res. 2015;27:437–49.
[154] Hodgkinson CL, Morrow CJ, Li Y, Metcalf RL, Rothwell DG, Trapani F, et al. Tumorigenicity and genetic profiling of circulating tumor cells in smallcell lung cancer. Nat Med. 2014;20:897–903.
[155] Barriere G, Fici P, Gallerani G, Fabbri F, Zoli W, Rigaud M. Circulating tumor cells and epithelial, mesenchymal and stemness markers: characterization of cell subpopulations. Ann Transl Med. 2014;2:109.
[156] Hayes DF, Cristofanilli M, Budd GT, Ellis MJ, Stopeck A, Miller MC, et al. Circulating tumor cells at each follow-up time point during therapy of metastatic breast cancer patients predict progression-free and overall survival. Clin Cancer Res. 2006;12(14 Pt 1):4218–24.
[157] de Bono JS, Scher HI, Montgomery RB, Parker C, Miller MC, Tissing H, et al. Circulating tumor cells predict survival benefit from treatment in metastatic castration-resistant prostate cancer. Clin Cancer Res. 2008;14:6302–9.
[158] Cohen SJ, Punt CJA, Iannotti N, Saidman BH, Sabbath KD, Gabrail NY, et al. Relationship of circulating tumor cells to tumor response, progression-free survival, and overall survival in patients with metastatic colorectal cancer. J Clin Oncol. 2008;26:3213–21.
[159] Hou JM, Krebs MG, Lancashire L, Sloane R, Backen A, Swain RK, et al. Clinical significance and molecular characteristics of circulating tumor cells and circulating tumor microemboli in patients with small-cell lung cancer. J Clin Oncol. 2012;30:525–32.
[160] Krebs MG, Hou JM, Sloane R, Lancashire L, Priest L, Nonaka D, et al. Analysis of circulating tumor cells in patients with non-small cell lung cancer using epithelial marker-dependent and -independent approaches. J Thorac Oncol. 2012;7:306–15.
[161] Crosbie PA, Shah R, Krysiak P, Zhou C, Morris K, Tugwood J, et al. Circulating tumor cells detected in the tumor-draining pulmonary vein are associated with disease recurrence after surgical resection of NSCLC. J Thorac Oncol. 2016;11:1793–7.
[162] Tanaka F, Yoneda K, Kondo N, Hashimoto M, Takuwa T, Matsumoto S, et al. Circulating tumor cell as a diagnostic marker in primary lung cancer. Clin Cancer Res. 2009;15:6980–6.
[163] Hofman V, Ilie MI, Long E, Selva E, Bonnetaud C, Molina T, et al. Detection of circulating tumor cells as a prognostic factor in patients undergoing radical surgery for non-small-cell lung carcinoma: comparison of the efficacy of the cell

search assay and the isolation by size of epithelial tumor cell method. Int J Cancer. 2011;129:1651–60.
[164] Ilie M, Hofman V, Mira EL, Selva E, Vignaud JM, Padovani B, et al. "Sentinel" circulating tumor cells allow early diagnosis of lung cancer in patients with chronic obstructive pulmonary disease. PLoS One. 2014;9:e111597.
[165] Lou J, Ben S, Yang G, Liang X, Wang X, Ni S, et al. Quantification of rare circulating tumor cells in non-small cell lung cancer by ligand targeted PCR. PLoS One. 2013;8:e80458.
[166] Campton DE, Ramirez AB, Nordberg JJ, Drovetto N, Clein AC, Varshavskaya P, et al. High-recovery visual identification and single-cell retrieval of circulating tumor cells for genomic analysis using a dual technology platform integrated with automated immunofluorescence staining. BMC Cancer. 2015;15:360.
[167] Belinsky SA, Liechty KC, Gentry FD, Wolf HJ, Rogers J, Vu K, et al. Promoter hypermethylation of multiple genes in sputum precedes lung cancer incidence in a high-risk cohort. Cancer Res. 2006;66:3338–44.
[168] Paggiaro PL, Chanez P, Holz O, Sterk PJ, Djukanovic R, Maestrelli P, et al. Sputum induction. Eur Respir J Suppl. 2002;20:3–8s.
[169] Nightingale JA, Rogers DF, Barnes PJ. Effect of repeated sputum induction on cell counts in normal volunteers. Thorax. 1998;53:87–90.
[170] Thunnissen FBJM. Sputum examination for early detection of lung cancer. J Clin Pathol. 2003;29(1):19–23.
[171] Horváth I, Barnes PJ, Loukides S, Sterk PJ, Högman M, Olin AC, et al. A European respiratory society technical standard: exhaled biomarkers in lung disease. Eur Respir J. 2017;49(4):1600965.
[172] Capuano R, Santonico M, Pennazza G, Ghezzi S, Martinelli E, Rosioni C, et al. The lung cancer breath signature: a comparative analysis of exhaled breath and air sampled from inside the lungs. Sci Rep. 2015;5:1–10.
[173] Corradi M, Poli D, Banda I, Bonini S, Mozzoni P, Pinelli S, et al. Exhaled breath analysis in suspected cases of non-smallcell lung cancer: a cross-sectional study. J Breath Res. 2015;9:27101.
[174] Li M, Yang D, Brock G, Knipp RJ, Bousamra M, Nantz MH, et al. Breath carbonyl compounds as biomarkers of lung cancer. Lung Cancer. 2015;90:92–7.
[175] Saalberg Y, Wolff M. VOC breath biomarkers in lung cancer. Clin Chim Acta. 2016;459:5–9.
[176] Bikov A, Hernadi M, Korosi BZ, Kunos L, Zsamboki G, Sutto Z, et al. Expiratory flow rate, breath hold and anatomic dead space influence electronic nose ability to detect lung cancer. BMC Pulm Med. 2014;14:202.
[177] Yu F, Choudhury D. Microfluidic bioprinting for organ-on-a-chip models. Drug Discov Today. 2019;24:1248–57.
[178] Sontheimer-Phelps A, Hassell BA, Ingber DE. Modelling cancer in microfluidic human organs-on-chips. Nat Rev Cancer. 2019;19:65–81.
[179] Xu Z, Li E, Guo Z, Yu R, Hao H, Xu Y, et al. Design and construction of a multi-organ microfluidic chip mimicking the in vivo microenvironment of lung cancer metastasis. ACS Appl Mater Interfaces. 2016;8(39):25840–7.
[180] Hao S, Ha L, Cheng G, Wan Y, Xia Y, Sosnoski DM, et al. A spontaneous 3d bone-on-a-chip for bone metastasis study of breast cancer cells. Small. 2018;4(12):1–10.
[181] Ribaut C, Voisin V, Malachovská V, Dubois V, Mégret P, Wattiez R, et al. Small biomolecule immunosensing with plasmonic optical fiber grating sensor. Biosens Bioelectron. 2016;77:315–22.
[182] Chiu NF, Lin TL, Kuo CT. Highly sensitive carboxyl-graphene oxide-based surface plasmon resonance immunosensor for the detection of lung cancer for cytokeratin 19 biomarker in human plasma. Sens Actuators, B Chem. 2018;265:264–72.
[183] Deng H, Liu Q, Wang X, Huang R, Liu H, Lin Q, et al. Quantum dots-labeled strip biosensor for rapid and sensitive detection of microRNA based on target-recycled nonenzymatic amplification strategy. Biosens Bioelectron. 2017;87:931–40.
[184] Soloducho J, Cabaj J. Electrochemical and optical biosensors in medical applications. In: Toonika R, editor. Biosensors–micro and nanoscale applications. London, UKL: IntechOpen; 2015. p. 321–46. ISBN 9789537619343.
[185] Hosu O, Selvolini G, Marrazza G. Recent advances of immunosensors for detecting food allergens. Curr Opin Electrochem. 2018;10:149–56.
[186] Ge S, Sun M, Liu W, Li S, Wang X, Chu C, et al. Disposable electrochemical immunosensor based on peroxidase-like magnetic silica-graphene oxide composites for detection of cancer antigen 153. Sens Actuators B Chem. 2014;192:317–26.
[187] Capuano R, Catini A, Paolesse R, Di Natale C. Sensors for lung cancer diagnosis. J Clin Med. 2019;8(2):235.
[188] Cheng S, Hideshima S, Kuroiwa S, Nakanishi T, Osaka T. Label-free detection of tumor markers using field effect transistor (FET)-based biosensors for lung cancer diagnosis. Sens Actuators, B Chem. 2015;212:329–34.
[189] Wu Y, Zhang H, Xiang J, Mao Z, Shen G, Yang F, et al. Ultrasensitive and high specific detection of non-small-cell lung cancer cells in human serum and clinical pleural effusion by aptamer-based fluorescence spectroscopy. Talanta. 2018;179:501–6.
[190] Zhao L, Tang C, Xu L, Zhang Z, Li X, Hu H, et al. Enhanced and differential capture of circulating tumor cells from lung cancer patients by microfluidic assays using aptamer cocktail. Small. 2016;12(8):1072–81.
[191] Kumar S, Umar M, Saifi A, Kumar S, Augustine S, Srivastava S, et al. Electrochemical paper based cancer biosensor using iron oxide nanoparticles decorated PEDOT:PSS. Anal Chim Acta. 2019;1056:135–45.
[192] Yu MK, Kim D, Lee IH, So JS, Jeong YY, Jon S. Image-guided prostate cancer therapy using aptamer-functionalized thermally cross-linked superparamagnetic iron oxide nanoparticles. Small. 2011;7(15):2241–9.
[193] Singh A, Kumar V. Iron oxide nanoparticles in biosensors, imaging and drug delivery applications–a complete tool. Intell Syst Ref Library. 2020;180:243–52.
[194] Wu Y, Wu H, Kuan C, Lin CJ, Wang LW, et al. Multi-functionalized carbon dots as theranosticnano agent for gene delivery in lung cancer therapy. Sci Rep. 2016;6:1–12.
[195] Alberti D, Protti N, Toppino A, Deagostino A, Lanzardo S, Bortolussi S, et al. A theranostic approach based on the use of a dual boron/Gd agent to improve the efficacy of boron neutron capture therapy in the lung cancer treatment. Nanomed Nanotech Biol Med. 2015;11:741–50.
[196] Wang Y, Zhang Y, Du Z, Wu M, Zhang G. Detection of micrometastases in lung cancer with magnetic nanoparticles and quantum dots. Int J Nanomed. 2012;7:2315–24.

[197] Maeda Y, Yoshino T, Matsunaga T. Novel nanocomposites consisting of in vivo-biotinylated bacterial magnetic particles and quantum dots for magnetic separation and fluorescent labeling of cancer cells. J Mater Chem. 2009;19(35):6361–6.
[198] Liang G, Fan W, Luo H, Zhu X. The emerging roles of artificial intelligence in cancer drug development and precision therapy. Biomed Pharmacother. 2020;128:110255.
[199] Kulski JK. Next generation sequencing: advances, applications and challenges (next-generation sequencing — an overview of the history, tools, and "omic" applications). London: IntechOpen; 2016.
[200] Jiang F, Jiang Y, Zhi H, Dong Y, Li H, Ma S, et al. Artificial intelligence in healthcare: past, present and future. Stroke Vasc Neurol. 2017;2(4):230–43.
[201] Davenport T, Kalakota R. The potential for artificial intelligence in healthcare. Future Healthc J. 2019;6(2):94–8.
[202] Robles AI, Harris CC. Integration of multiple "OMIC" biomarkers: a precision medicine strategy for lung cancer. Lung Cancer. 2017;107:50–8.
[203] Nicora G, Vitali F, Dagliati A, Geifman N, Bellazzi R. Integrated multi-omics analyses in oncology: a review of machine learning methods and tools. Front Oncol. 2020;10:1030.
[204] Holzinger A, Kains BH, Jurisica I. Why imaging data alone is not enough: AI-based integration of imaging, omics, and clinical data. Eur J Nucl Med Mol Imaging. 2019;46:2722–30.
[205] Lo Gullo R, Daimiel I, Morris EA, Pinker K. Combining molecular and imaging metrics in cancer: radiogenomics. Insights Imaging. 2020;11:1.
[206] Song L, Zhu Z, Wu H, Han W, Cheng X, Li J, et al. Individualized nomogram for predicting ALK rearrangement status in lung adenocarcinoma patients. Eur Radiol. 2021;31(4):2034–47.
[207] Rizzo S, Petrella F, Buscarino V, De Maria F, Raimondi S, Barberis M, et al. CT radiogenomic characterization of EGFR, K-RAS, and ALK mutations in non-small cell lung cancer. Eur Radiol. 2016;26:32–42.
[208] ITU. Measuring the information society Report 2014. Int Commun Union 2014.
[209] Jin H, Huynh TP, Haick H. Self-healable sensors based nanoparticles for detecting physiological markers via skin and breath: toward disease prevention via wearable devices. Nano Lett. 2016;16:4194–202.
[210] Cannon C. Telehealth, mobile applications, and wearable devices are expanding cancer care beyond walls. Semin Oncol Nurs. 2018;34:1–8.
[211] Cancer research UK. App launched to help doctors assess risk of lung cancer in people with lung nodules. Press release; 2016. Available from: https://www.cancerresearchuk.org/about-us/cancer-news/press-release/2016-12-06applaunched- to-help-doctors-assess-risk-of-lung-cancer-in-people-with-lung-nodules.
[212] Ji D, Liu Z, Liu L, Low SS, Lu Y, Yu X, et al. Smartphone-based integrated voltammetry system for simultaneous detection of ascorbic acid, dopamine, and uric acid with graphene and gold nanoparticles modified screen-printed electrodes. Biosens Bioelectron. 2018;119:55–62.